Eustatic variations during the Paleocene-Eocene greenhouse world

Appy Sluijs,[1] Henk Brinkhuis,[1] Erica M. Crouch,[2] Cédric M. John,[3,4] Luke Handley,[5] Dirk Munsterman,[6] Steven M. Bohaty,[3] James C. Zachos,[3] Gert-Jan Reichart,[7] Stefan Schouten,[8] Richard D. Pancost,[5] Jaap S. Sinninghe Damsté,[7,8] Natasja L. D. Welters,[1] André F. Lotter,[1] and Gerald R. Dickens[9]

Received 5 March 2008; revised 5 September 2008; accepted 16 September 2008; published 19 December 2008.

[1] We reconstruct eustatic variations during the latest Paleocene and earliest Eocene (~58–52 Ma). Dinoflagellate cysts, grain size fractions, and organic biomarkers in marine sections at four sites from three continents indicate an increased distance to the coast during the Paleocene-Eocene thermal maximum (PETM). The same trend is recognized in published records from other sites around the world. Together, the data indicate a eustatic rise during the PETM, beginning 20 to 200 ka before the globally recorded negative carbon isotope excursion (CIE) at ~55.5 Ma. Although correlations are tentative, we recognize other global transgressions during Chrons C25n and C24n. The latter may be associated with Eocene Thermal Maximum 2 (~53.5 Ma) or the ''X''-event (~52 Ma). These results suggest a link between global sea level and ''hyperthermal'' intervals, potentially because of the melting of small alpine ice sheets on Antarctica, thermal expansion of seawater, or both. However, the early onset of sea level rise relative to the CIE of the PETM suggests contributions from other mechanisms, perhaps decreasing ocean basin volume, on sea level rise.

Citation: Sluijs, A., et al. (2008), Eustatic variations during the Paleocene-Eocene greenhouse world, *Paleoceanography*, *23*, PA4216, doi:10.1029/2008PA001615.

1. Introduction

[2] Earth's surface warmed by about 5°C from the late Paleocene (~59 Ma) through the early Eocene Climatic Optimum (EECO; 52–50 Ma) [*Zachos et al.*, 2001]. Superimposed on this long-term warming trend were at least two hyperthermals (brief (<200 ka) intervals characterized by anomalously high temperatures [*Bowen et al.*, 2006; *Sluijs et al.*, 2007a] (Figure 1)). The Paleocene-Eocene Thermal Maximum (PETM; ~55.5 Ma), the most prominent and best studied, was characterized by a global rise of 5–8°C [e.g., *Kennett and Stott*, 1991; *Zachos et al.*, 2003; *Sluijs et al.*, 2006]. A less pronounced hyperthermal occurred at ~53.6 Ma referred to as H–1, Eocene Thermal Maximum 2 (ETM2) or ''Elmo'' [*Lourens et al.*, 2005]; other ones possibly occurred at ~53.2 Ma (I–1) and at ~52.4 Ma (K or X) [*Cramer et al.*, 2003; *Röhl et al.*, 2005; *Nicolo et al.*, 2007]. These Eocene hyperthermals, both documented (PETM, ETM2) and suspected (I and K), are marked by prominent negative carbon isotope excursions in sedimentary components and carbonate dissolution in deep-sea sediment records [*Lourens et al.*, 2005; *Röhl et al.*, 2005; *Zachos et al.*, 2005]. These observations are consistent with rapid, massive injections of ^{13}C-depleted carbon into the ocean-atmosphere system, although the mechanism for such release remains controversial [*Dickens et al.*, 1995; *Higgins and Schrag*, 2006; *Sluijs et al.*, 2007a].

[3] The character of global sea level change (or eustacy) during the late Paleocene and early Eocene has direct relevance to the origin of hyperthermals. Two proposed causes for the hyperthermals (oxidation of organic matter in subaerially exposed marine deposits [*Higgins and Schrag*, 2006]; release of microbially derived methane from the shelf [*Schmitz et al.*, 2004]) invoke a significant drop in sea level. A third proposed cause, mantle plume initiated volcanism in the north Atlantic [*Svensen et al.*, 2004], should have caused a rise. Constraints on the rate, magnitude and timing of sea level change are key to testing these hypotheses.

[4] Early Cenozoic warmth at high latitudes would have precluded development of large continental ice sheets [e.g., *DeConto and Pollard*, 2003]. Indeed, the unusually low oxygen isotopic ratios of late Paleocene-early Eocene benthic foraminiferal calcite (0–1‰) suggest little ice, even after accounting for warm bottom water temperatures [*Miller et al.*, 1987; *Zachos et al.*, 2001]. With limited continental ice and average deep ocean temperatures of 8–15°C, early

[1]Palaeoecology, Institute of Environmental Biology, Laboratory of Palaeobotany and Palynology, Utrecht University, Utrecht, Netherlands.
[2]GNS Science, Lower Hutt, New Zealand.
[3]Earth and Planetary Sciences Department, University of California at Santa Cruz, California, USA.
[4]Now at Department of Earth Science and Engineering, Imperial College London, London, UK.
[5]Bristol Biogeochemistry Research Centre, Organic Geochemistry Unit, School of Chemistry, University of Bristol, Bristol, UK.
[6]Netherlands Institute of Applied Geoscience TNO–National Geological Survey, Utrecht, Netherlands.
[7]Department of Earth Sciences, Utrecht University, Utrecht, Netherlands.
[8]Department of Marine Biogeochemistry and Toxicology, Royal Netherlands Institute for Sea Research, Den Burg, Texel, Netherlands.
[9]Department of Earth Science, Rice University, Houston, Texas, USA.

Copyright 2008 by the American Geophysical Union.
0883-8305/08/2008PA001615

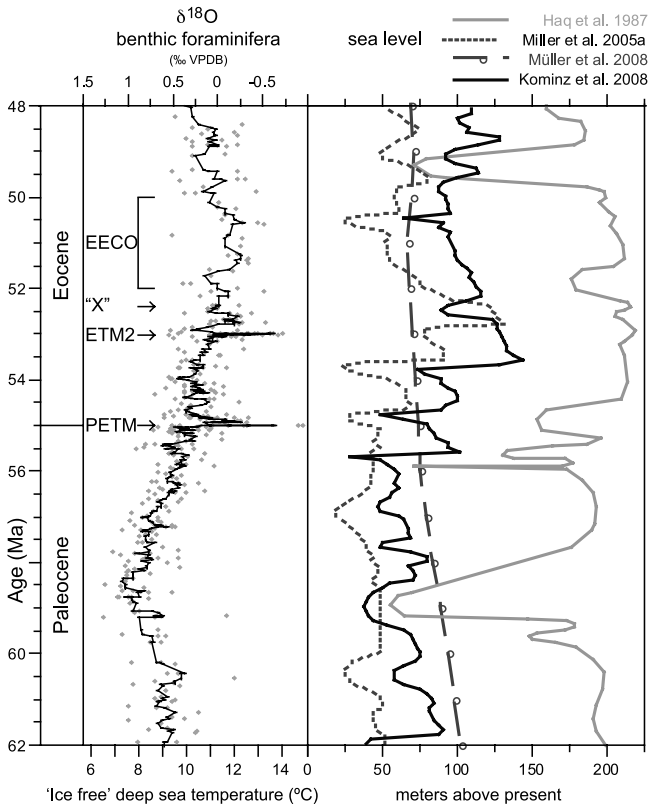

Figure 1. Comparison of deep-sea benthic foraminifer $\delta^{18}O$ and sea level records between 62–48 Ma. Gray diamonds represent corrected $\delta^{18}O$ values compiled by *Zachos et al.* [2001] complemented with the *Cibicidoides* data for ETM2 from *Lourens et al.* [2005]. An additional correction of −0.25 ‰ was applied to the Eocene Thermal Maximum 2 (ETM2) *Cibicidoides* values to synchronize baseline levels between the records. Black line is a five-point moving average. Temperature scale is based on the assumption that no continental ice prevailed. Sea level curves are from *Haq et al.* [1987], *Miller et al.* [2005a], *Kominz et al.* [2008], and *Müller et al.* [2008]. *Müller et al.* [2008] represents variations in ocean basin volume in meters of sea level assuming no ice sheets and a constant volume of ocean water. EECO, early Eocene Climatic Optimum (52–50 Ma [*Zachos et al.*, 2001]); PETM, Paleocene-Eocene Thermal Maximum; VPDB, Vienna Pee Dee Belemnite.

Paleogene sea level should have been 70–80 m higher than present-day, assuming a similar volume for the overall ocean basin, or upward of 120 m higher than present-day, if this volume was significantly smaller [*Müller et al.*, 2008]. However, small ice sheets may have existed on elevated regions of Antarctica throughout the early Paleogene, and these could have contributed to low-amplitude sea level variations [*Miller et al.*, 1998a; *Speijer and Wagner*, 2002; *DeConto and Pollard*, 2003; *Miller et al.*, 2005b]. Thermal expansion and contraction of ocean water may also have affected sea level by several meters given the temperature-density relationship of seawater ($1.9 \cdot 10^{-4}$ $m^3/°T$). Although refuting certain causes for the hyperthermals, long-term and short-term highs in sea level, albeit of low amplitude, might coincide with the temperature extremes of the EECO and hyperthermals, respectively.

[5] The timing and amplitude of early Cenozoic sea level variations can be assessed through analyses of sedimentary packages deposited on continental margins (i.e., sequence stratigraphy) [*Mitchum et al.*, 1977; *Vail et al.*, 1977; *Haq et al.*, 1987]. During a sea level cycle, the sediment depocenter as well as grain size and composition of the sediments varies. During lowstands, accommodation space may be too small on the shelf to accumulate sediments. During highstands, thick sequences may accumulate with sufficient terrigenous sediment influx, and the grain size and composition of the sediments is then dependent on the distance to the source of sediment input [*Mitchum et al.*, 1977; *Vail et al.*, 1977; *Miller et al.*, 1998a]. On the basis of sequences from continental slopes, early work suggested that late Paleocene and early Eocene sea level fluctuated between 50 and 220 m higher than at present [*Haq et al.*, 1987]. This work also inferred large amplitude variations on short time intervals ($<10^6$ a), including a 40 m drop near the Paleocene-Eocene Boundary (Figure 1). More recent work, especially on the New Jersey margin, has included "backstripping", which accounts for sediment compaction and loading [*Kominz et al.*, 1998; *Miller et al.*, 1998a; *van Sickel et al.*, 2004; *Miller et al.*, 2005a]. In general, these studies indicate that sea level was 70–140 m higher during the late Paleocene and early Eocene than at present. Third-order sea level cycles, with durations of hundreds of thousands to a few million years, have also been inferred and argued to represent eustatic variations [e.g., *Haq et al.*, 1987; *Speijer and Wagner*, 2002; *Miller et al.*, 2005a] (Figure 1).

[6] Although recent sea level curves [*Miller et al.*, 2005a] are closer to general expectations [*Müller et al.*, 2008], some key uncertainties still exist, particularly regarding higher-order cycles. First, peak Cenozoic sea level appears to occur >1 Ma before the EECO and maximum Cenozoic temperatures (Figure 1). Second, given the low temporal resolution of the curves, it is not clear whether some of the sea level highs correspond to hyperthermals. In most cases, the sequences underlying the sea level reconstructions have not been directly calibrated to the PETM, ETM-2 and other suspected hyperthermals using carbon isotope stratigraphy. In the few cases where such stratigraphy exists, the magnitude and direction of the sea level change has been controversial. In particular, some authors [*Schmitz et al.*, 2001; *Schmitz and Pujalte*, 2003; *Schmitz et al.*, 2004] have argued that lithological changes across the PETM support a major sea level fall, whereas in other cases microfossil and geochemical data has been used to suggest the opposite trend [*Sluijs et al.*, 2006, 2008]. One recently acknowledged problem is that sediment supply to continental margins varied significantly during the early Paleogene, especially across the hyperthermals [e.g., *Nicolo et al.*, 2007; *Sluijs et al.*, 2008] (Figure 2), and this could influence stratigraphic interpretations [*Vail et al.*, 1977; *Steckler et al.*, 1988].

[7] Here, we address eustacy through the late Paleocene and early Eocene, particularly during the PETM, by exam-

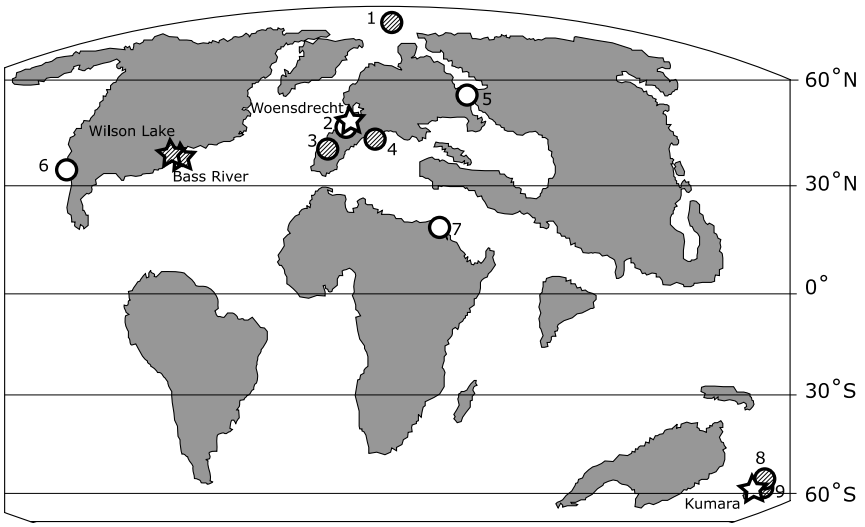

Figure 2. Location of the studied sites within a paleogeographic reconstruction of the Earth at PETM times; modified from *Scotese and Golanka* [1992]. Stars indicate locations from which new data are presented. Circles indicate marginal marine PETM sites with published information on late Paleocene-early Eocene sea level (SL). Symbols filled with stripes indicate marginal marine sites for which published information has indicated an increase in terrigenous sediment supply (TS) during the PETM or other hyperthermals. Increase in terrigenous sediment supply for Bass River and Wilson Lake is from *Sluijs et al.* [2007b] and *John et al.* [2008]. Numbers refer to the following sites: site 1, Lomonosov Ridge, Arctic Ocean (SL, TS [*Sluijs et al.*, 2006, 2008]); site 2, Doel, North Sea (SL [*Steurbaut et al.*, 2003]); site 3, Basque Region, Bay of Biscay (SL, TS [*Schmitz et al.*, 2001; *Pujalte and Schmitz*, 2006]); site 4, Forada, Central Northern Tethys (TS [*Giusberti et al.*, 2007]); site 5, Turgay Straight (SL [*Iakovleva et al.*, 2001]); site 6, Lodo Formation, California (SL [*John et al.*, 2008]); site 7, Gebel Duwi, Central Southern Tethys (SL [*Speijer and Morsi*, 2002]); site 8, Tawanui, Southwestern Pacific (TS [*Crouch et al.*, 2003b], SL [*Crouch and Brinkhuis*, 2005]); and site 9, Clarence River Valley, Southwestern Pacific (TS PETM [*Hollis et al.*, 2005], TS other presumed hyperthermals [*Nicolo et al.*, 2007]).

ining variations in sedimentary components from sites located on past margins of several ocean basins. In general, the chosen components, including dinoflagellate cysts (dinocysts), influx of terrestrial organic matter and grain size, are proxies for distance to the coast.

2. Sea Level Indicators

[8] Sedimentary components often change across modern shelves in relation to coastal proximity. Physio-chemical parameters vary greatly across the shelf and upper slope because of numerous factors, including upwelling, freshwater and nutrient discharge from rivers, and turbidity. With a rise (or fall) in sea level, therefore, sedimentary components at a specific site might become more characteristic of offshore (or inshore) settings and serve as a means to reconstruct water depth. For example, the distribution of benthic foraminifera and ostracodes as well as the relative abundance of planktonic versus benthic foraminifera have been used to study late Paleocene and early Eocene sea level variations along northern Africa [*Speijer and Schmitz*, 1998; *Speijer and Morsi*, 2002; *Speijer and Wagner*, 2002]. Along with eustacy, however, such records may be influenced by local changes in water depth. To elucidate eustatic variations, independent proxies should be examined at multiple sections along widely separated continental margins.

[9] Organic dinoflagellate cysts (dinocysts) are produced by dinoflagellates for the dormant stage of their life cycle and behave as silt-sized sedimentary particles [*Fensome et al.*, 1996]. The dinoflagellates that make the cysts inhabit surface waters, dominantly in marginal marine settings [*Wall et al.*, 1977; *Bradford and Wall*, 1984; *Fensome et al.*, 1996]. The nearshore setting is also where dinocyst preservation is best because shallow sediments are often reduced. Individual species are very sensitive to differences in surface water properties [*Taylor*, 1987; *Dale*, 1996]. Consequently, dinocyst assemblages exhibit systematic variation across the seafloor from the coast to open water [*Wall et al.*, 1977; *Harland*, 1983; *Bradford and Wall*, 1984; *Marret and Zonneveld*, 2003]. This inshore-offshore variance has been documented in sediment deposited across continental margins of the past, including the Paleogene when shelf areas were more expansive than at present [*Köthe*, 1990; *Brinkhuis*, 1994; *Pross and Brinkhuis*, 2005]. Dinocyst assemblage records have also been employed to reconstruct the relative influence of near shore and offshore waters, and thereby sea level fluctuations, throughout the Cenozoic [*Brinkhuis*, 1994; *Powell et al.*, 1996; *Röhl et al.*,

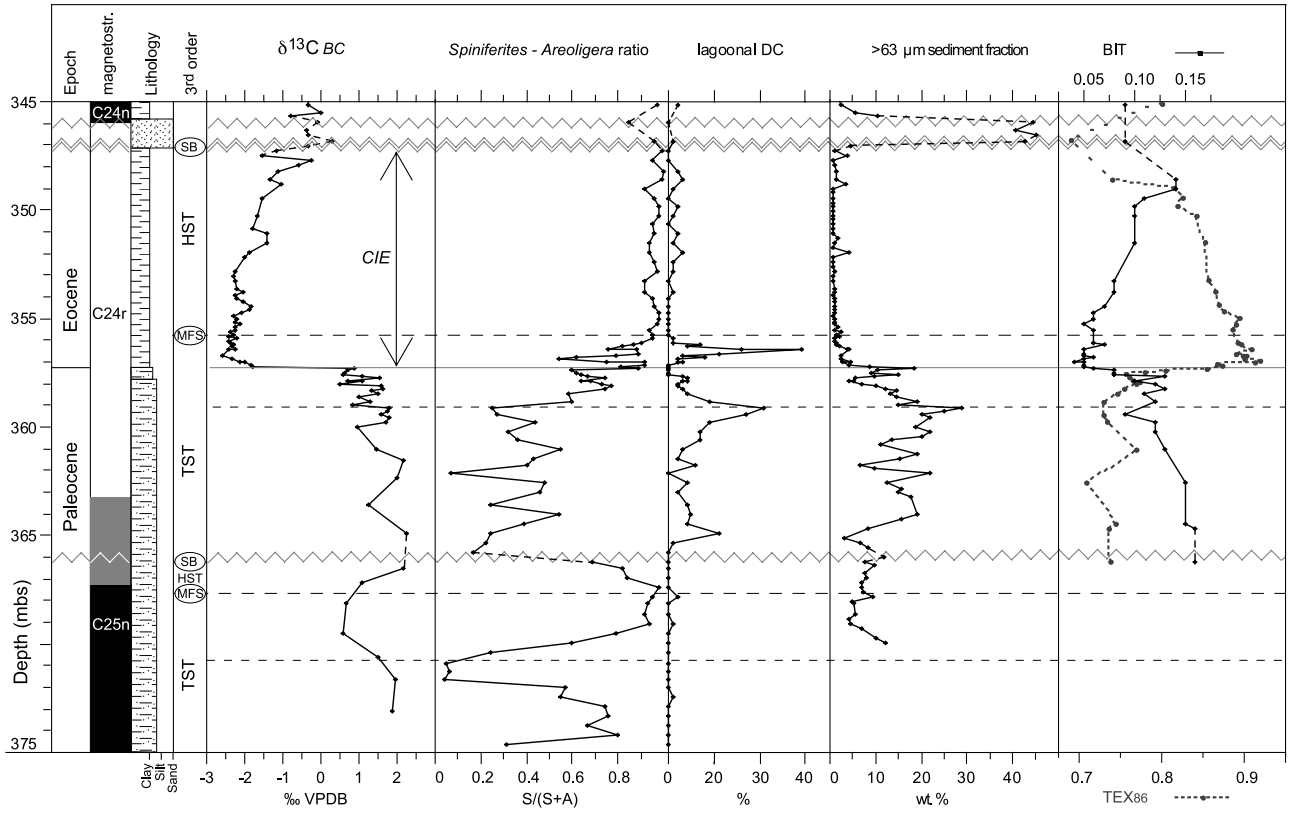

Figure 3. Bass River, New Jersey: magnetostratigraphy, sequence stratigraphic interpretation, bulk carbonate (BC) $\delta^{13}C$ from *John et al.* [2008], TEX_{86} record from *Sluijs et al.* [2007b], *Spiniferites*/*Areoligera* ratio, percentage lagoonal dinocysts (DC), percent sand data, and BIT index through the latest Paleocene-earliest Eocene. Paleomagnetic data are from *Cramer et al.* [1999]. mbs, meters below surface; SB, Sequence Boundary; MFS, maximum flooding surface; HST, Highstand Systems Tract; TST, Transgressive Systems Tract.

2004; *Pross and Brinkhuis*, 2005; *Sluijs et al.*, 2005; *Torricelli et al.*, 2006], including the late Paleocene and early Eocene [*Powell et al.*, 1996; *Bujak and Brinkhuis*, 1998; *Crouch and Brinkhuis*, 2005]. High-resolution dinocyst-based sea level records across hyperthermals, however, have been limited to New Zealand [*Crouch and Brinkhuis*, 2005], and the North Sea [*Powell et al.*, 1996]. These studies did not examine other independent proxies to confirm results.

[10] There are other means to assess variations in coastal proximity. One is the relative abundance of terrestrially derived palynomorphs (pollen and spores), which are dominantly supplied by rivers. Generally, the relative abundances of terrestrial palynomorphs increase closer to shore. Another is the Branched and Isoprenoid Tetraether (BIT) index [*Hopmans et al.*, 2004]. This measures the relative amount of terrestrially derived branched tetraether lipids, relative to marine-derived isoprenoid tetraether lipids. Hence, as with terrestrial palynomorphs, the BIT index should increase closer to the coast [*Hopmans et al.*, 2004]. Finally, large grains are deposited closer to shore than small grains when they are transported from land to the ocean. The size fraction >63 μm (wt. % sand) thus provides another means of identifying sequence boundaries. It should be noted that all these proxies are also influenced by variations in river runoff.

3. Sites and Samples

3.1. Bass River and Wilson Lake, New Jersey Shelf

[11] Ocean Drilling Program Leg 174AX Site "Bass River" [*Miller et al.*, 1998b] and United States Geological Survey (USGS) borehole "Wilson Lake" are located in southern New Jersey (United States). Cores from both sites contain upper Paleocene-lower Eocene sediments deposited on a broad continental shelf (Figure 2) [*Gibson et al.*, 1993], perhaps as far south as ~27°N [*Kopp et al.*, 2007]. Average paleowater depth at Bass River has been estimated at ~150 m, on the basis of benthic foraminifer assemblages [*van Sickel et al.*, 2004]. At Wilson Lake, late Paleocene-early Eocene water depth was probably similar to that at the nearby Ancora section, which was ~50 m on the basis of benthic foraminifer assemblages [*van Sickel et al.*, 2004]. Even though Cenozoic subsidence of New Jersey has been underestimated in backstripping studies [*Müller et al.*, 2008], regional tectonics should have had minor influence on sea level variations in the late Paleocene-early Eocene, with subsidence primarily controlled by simple lithospheric

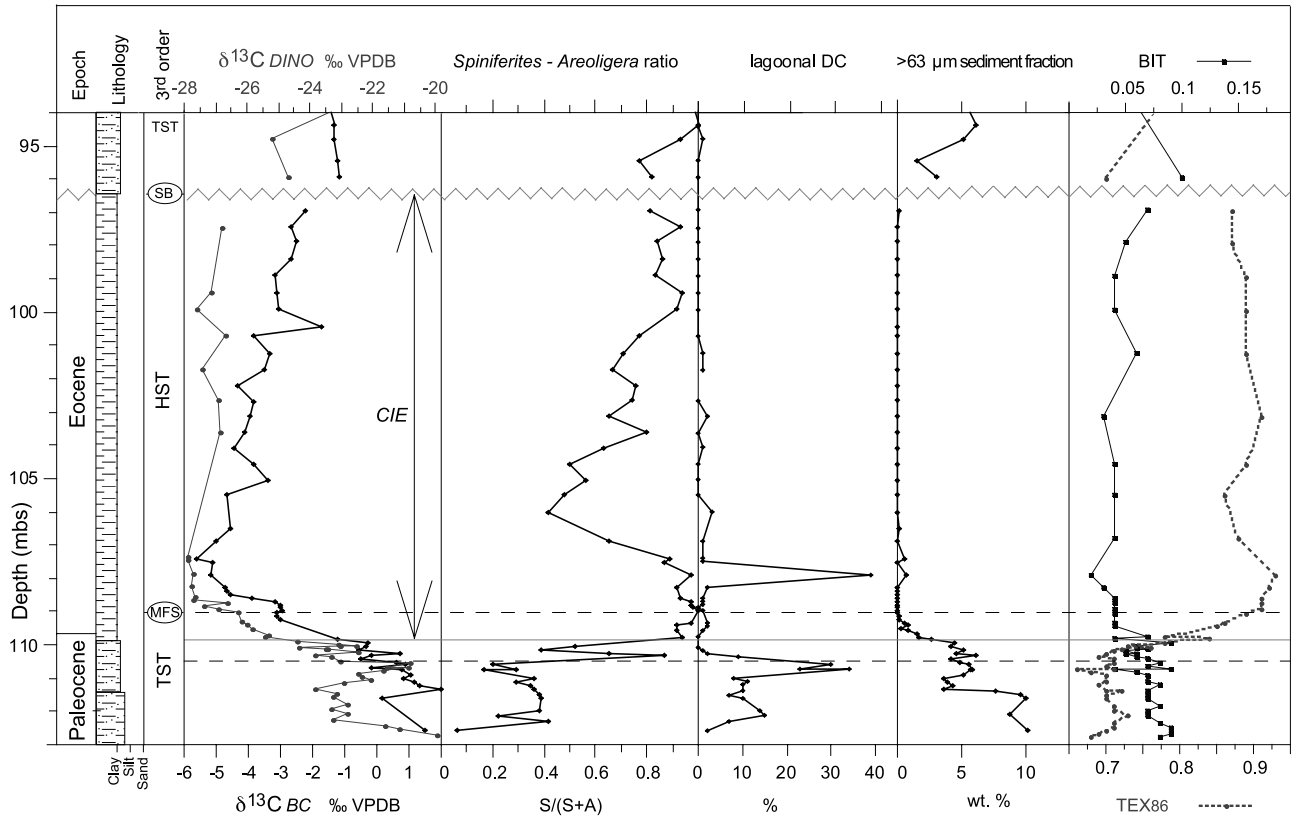

Figure 4. Wilson Lake, New Jersey: sequence stratigraphic interpretation, BC, and dinocyst (DINO) δ^{13}C records and TEX_{86} data (data all from *Sluijs et al.* [2007b]), *Spiniferites*/*Areoligera* ratio, percentage lagoonal DC, percent sand, and BIT index data through the latest Paleocene-earliest Eocene.

cooling, compaction and loading [*Miller*, 1997; *Miller et al.*, 1998b, 2004]. Consequently, sediment deposition across the shelf and at these sites should have been influenced by changes in eustacy.

[12] The age models at Bass River and Wilson Lake are based on calcareous nannofossil biostratigraphy, and identification of the carbon isotope excursion (CIE) [*Cramer et al.*, 1999; *Sluijs et al.*, 2007b] (Figure 3). Additionally, paleomagnetic analyses have been carried out at Bass River [*Cramer et al.*, 1999]. At Bass River, a relatively complete uppermost Paleocene is present between ~375 and 357.3 meters below surface (mbs). The Chron C25n-C24r boundary was defined with data having poor demagnetization patterns [*Cramer et al.*, 1999], so that its location could be in error by several meters. Still, the brief Chron C25n (~0.5 Ma; [*Westerhold et al.*, 2007]) appears expanded relative to the very long and condensed interval between the onset of C24n and the CIE (~1.3 Ma) (Figure 3). The CIE has been identified between 357.3 and ~347 mbs from δ^{13}C records on multiple carbon bearing phases [*Cramer et al.*, 1999; *Sluijs et al.*, 2007b; *John et al.*, 2008]. At Wilson Lake (Figure 4), the CIE has been identified between ~110.0 and ~96 mbs from δ^{13}C records on multiple carbon bearing phases [*Gibbs et al.*, 2006; *Zachos et al.*, 2006; *Sluijs et al.*, 2007b].

[13] At both Bass River and Wilson Lake, the CIE spans a clay-rich interval that overlies an uppermost Paleocene glauconite-rich sandy unit. At both sites, the upper part of the PETM is truncated by an unconformity associated with a glauconite-rich sand unit [*Cramer et al.*, 1999; *Gibbs et al.*, 2006]. Sediments above this sequence boundary are placed within Chron C24n, ~2 Ma younger than the PETM [*Lourens et al.*, 2005; *Westerhold et al.*, 2007], on the basis of nannofossil biostratigraphy and magnetostratigraphy [*Cramer et al.*, 1999; *Gibbs et al.*, 2006].

[14] Using the stratigraphic thickness of the CIE and its estimated duration of ~170 ka [*Röhl et al.*, 2007; *Sluijs et al.*, 2007a; *Abdul Aziz et al.*, 2008], average sedimentation rates can be calculated for both New Jersey sites. At Bass River, the first ~100 ka of the PETM (the upper part is truncated in the overlaying sequence boundary) is represented in ~10 m of section between 357 and 347 m [*Sluijs et al.*, 2007b], implying sedimentation rates of ~10 cm/ka. Using a similar approach, sedimentation rates across the PETM at Wilson Lake (110−96 m) have been estimated at 8.4 cm/ka [*Gibbs et al.*, 2006]. Sedimentation rates for the underlying glauconite-rich unit were much lower, perhaps one order of magnitude [*Sluijs et al.*, 2007b]. The above estimates represent average sedimentation rates, which may have varied substantially around the CIE, especially if sea level varied.

3.2. Woensdrecht, North Sea

[15] An upper Paleocene-lower Eocene succession was recovered in 1912 from a borehole (WDR-01) near the town of Woensdrecht in the Netherlands and was deposited on the southeastern shelf of the North Sea [*Dienst der Rijksopsporing van Delfstoffen*, 1918]. Upper Paleocene-lower Eocene strata composed of fine sands to clays [*Dienst der Rijksopsporing van Delfstoffen*, 1918] were identified using dinocyst biostratigraphy [*Munsterman*, 2004] (Figure 5a). The occurrence of the taxon *Apectodinium augustum*, which is diagnostic for the PETM [*Bujak and Brinkhuis*, 1998; *Steurbaut et al.*, 2003; *Sluijs et al.*, 2007b], marks the location of the PETM between 626 and 610 mbs.

3.3. Kumara-2, New Zealand

[16] The Kumara-2 core was drilled on the west coast of South Island ~15 km south of Greymouth. In the lower 50 m of core, between 1750 and 1700 mbs, Paleocene and Eocene sandstones, mudstones and coals [*Raine*, 1984; *Carter et al.*, 1986] with abundant but highly variable organic matter contents were recovered [*Pancost et al.*, 2006]. Most of the rocks are terrestrial, originally deposited in backswamp, overbank and channel environments, however, marine sediments deposited on the shelf are recognized from ~1739 to 1734 mbs [*Carter et al.*, 1986].

4. Methods

4.1. Palynological Methods

4.1.1. Processing

[17] Palynological processing of samples from the New Jersey and Woensdrecht sites was performed using standard methods based on HCl and HF treatment of the samples [cf. *Sluijs et al.*, 2003]. Processing techniques of samples from Kumara-2 were similar to those described above but used slightly different concentrations of acid and a narrower mesh sieve [*Crouch et al.*, 2003b]. The slight differences in processing should not have biased the resulting assemblages. We follow the dinocyst taxonomy of *Fensome and Williams* [2004].

4.1.2. Dinocysts as Indicators of Coastal Proximity

[18] Cyst-forming dinoflagellates dominantly comprise two types since the Triassic: the Gonyaulacales and the Peridiniales [*Fensome and Williams*, 2004]. Following previous studies that use dinocyst assemblages to reconstruct changes in proximity to the coast [e.g., *Brinkhuis*, 1994; *Pross and Brinkhuis*, 2005; *Sluijs et al.*, 2005], we use the relative abundance of Gonyaulacoid dinocyst taxa. The distribution of Peridinioid dinoflagellates is less sensitive to coastal proximity, as they are relatively euryhaline and react predominantly to changes in food supply [e.g., *Harland*, 1973; *Dale*, 1996]. In our samples, the Gonyaulacoid fraction is dominated by the *Areoligera* complex (cpx) and the *Spiniferites* cpx. *Areoligera* cpx has high relative abundances in inner neritic environments, whereas *Spiniferites* cpx. has higher relative abundances in outer neritic environments [*Brinkhuis*, 1994; *Marret and Zonneveld*, 2003; *Pross and Brinkhuis*, 2005; *Torricelli et al.*, 2006]. We use the S/A index (*Spiniferites*/(*Spiniferites* + *Areoligera*)) to quantify the abundances of the two complexes, with the assumption that low S/A represents an inner neritic setting, while high S/A indicates an outer neritic setting. Although *Spiniferites* abundance varies in our records, most fluctuations in the S/A index are due to variations in *Areoligera* abundance. In addition, we use the abundance of members of the Goniodomaceae family, here represented by *Eocladopyxis* and *Polysphaeridium* spp. These taxa are tolerant to highly variable salinities and are mainly recorded in lagoons and coastal margins [*Bradford and Wall*, 1984; *Brinkhuis*, 1994; *Reichart et al.*, 2004; *Pross and Brinkhuis*, 2005].

4.2. Organic Geochemistry

4.2.1. Stable Carbon Isotopes

[19] For stable carbon isotope analyses on total organic carbon ($\delta^{13}C_{TOC}$), samples from the Woensdrecht core were freeze dried, powdered and analyzed with a Fison NA 1500 CNS analyzer coupled to a Finnigan Delta Plus mass spectrometer. Analytical precision and accuracy were determined by replicate analyses and by comparison with international and in-house standards, and were better than 0.1% and 0.1‰, respectively.

[20] For C_{29} *n*-alkane carbon isotope ($\delta^{13}C_{n\text{-}C29}$) values, samples from Kumara-2 were washed with methanol, freeze dried and powdered. Powders were extracted using a Soxhlet apparatus for 24 hours using dichloromethane/methanol (2:1 v/v) as the organic solvent. Extracts were separated using an aminopropyl column by elution with DCM/isopropanol (3:1 v/v) and 2% (by volume) acetic acid in diethyl ether, to yield the neutral and acid fractions, respectively. Neutral fractions were further separated by an Al_2O_3 column, using hexane/DCM (9:1) and DCM/methanol (1:2) to yield the apolar and polar fractions, respectively. $\delta^{13}C_{n\text{-}C29}$ values were obtained from the apolar fraction using a Varian 3400 GC coupled to a Finnigan MAT Delta-S IRMS via an extensively modified Finnigan MAT Type I combustion interface.

[21] Carbon isotope values are reported relative to the Vienna Pee Dee Belemnite (VPDB) standard.

4.2.2. BIT Index

[22] For the Wilson Lake and Bass River cores, we generated BIT index data. Powdered and freeze-dried sediments (~20 g dry mass) were extracted with DCM/methanol (9:1) by using a Dionex ASE. The extracts were separated by Al_2O_3 column chromatography using hexane/DCM (9:1) and DCM/methanol (1:1) to yield the apolar and polar fractions, respectively. Polar fractions were filtered and analyzed using high-performance liquid chromatography/atmospheric pressure chemical ionization-mass spectrometry. Single ion monitoring was used to quantify the abundances of glycerol dialkyl glycerol tetraether (GDGT) lipids, used to calculate the BIT index. See *Hopmans et al.* [2004] for a more extensive description of the methods.

5. Results and Discussion

5.1. New Sites

5.1.1. New Jersey Shelf

[23] Palynomorphs are abundant and well preserved throughout the Bass River and Wilson Lake records. Dino-

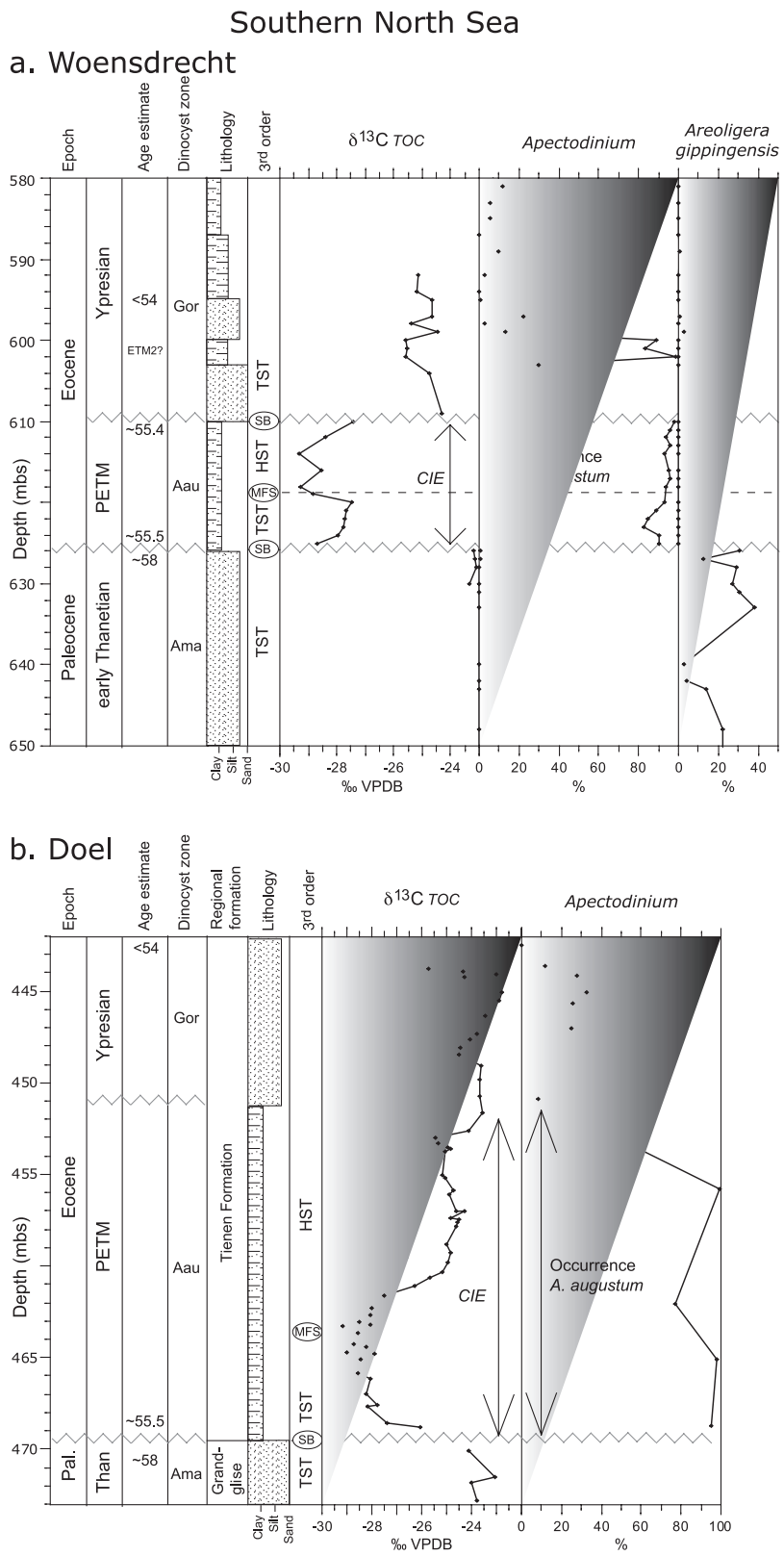

Figure 5. (a) Woensdrecht and (b) Doel, North Sea: sequence stratigraphic interpretation, total organic carbon (TOC) $\delta^{13}C$, abundance of dinocyst taxa *Apectodinium* spp. (including *A. augustum*), and *Areoligera gippingensis* (see text). Data from Doel are all from *Steurbaut et al.* [2003]. Dinocyst zones are adapted from *Powell* [1992] and *Powell et al.* [1996]. Ama, *Alisocysta margarita* zone; Aau, *Apectodinium augustum* zone; Gor, *Glaphyrocysta ornata* zone.

cysts outnumber other palynomorphs, and among them, *Apectodinium*, *Areoligera* and *Spiniferites* spp. are most abundant. In addition, representatives of peridinioid genera such as *Senegalinium* spp. are abundant over short intervals [*Sluijs et al.*, 2007b]. Terrestrial palynomorph abundances are low (<1%) and were not analyzed to significant numbers. BIT index values are generally low, but show reproducible fluctuations.

[24] At Bass River, an increase in the S/A index, within Chron C25n at 370 mbs, points to a greater distance between the site and the coast (Figure 3). The same interval is marked by a decreasing amount of sand, which comprises reworked glauconite in this part of the section [*Cramer et al.*, 1999]. Both observations suggest transgression. The interval between the top of Chron C25n and the CIE (~367–357 mbs) spans ~1.3 Ma [*Westerhold et al.*, 2007]. This implies sedimentation rates of less than 1 cm/ka, much lower than those of typical neritic sites or for the overlying PETM interval. Hence, this interval represents an extremely condensed section, and/or has a hiatus near the base [*Liu et al.*, 1997]. We infer a third-order sequence boundary at ~366 mbs, where there is a major decrease in the S/A index and an onset of lagoonal dinocysts (Figure 3). This interval, however, is not accompanied by a sharp break in lithology, but this could be explained by extensive bioturbation. Detailed biostratigraphic constraints are not available to estimate the duration of the hiatus associated with the sequence boundary, but considering the thin interval spanning Chron C24r below the CIE, it may be in the order of several hundreds of thousands of years. During the subsequent transgressive systems tract (TST; starting at ~366 mbs), which has been identified previously on the basis of lithological properties such as increasing grainsize (Figure 3) [*Liu et al.*, 1997; *Cramer et al.*, 1999], the BIT index gradually decreases while the S/A index gradually increases.

[25] The S/A index increases significantly between ~359 and 355 mbs at Bass River (Figure 3). In addition, the % lagoonal taxa and wt. % sand decreases (the sand again composed mostly of reworked glauconite [*Cramer et al.*, 1999]) and the BIT index is low. Together, these observations suggest a drop in energy levels and a decrease in the supply of terrestrial organic carbon; they are consistent with a transgression. The onset of this transgression occurred even prior to the beginning of PETM-related warming at ~357.5 mbs just below the CIE [*Sluijs et al.*, 2007b]. We place the maximum flooding surface (mfs) at ~355 mbs, where the S/A index is at a maximum, and the wt. % sand and BIT index are at minima. This interval coincides with the uppermost occurrence of glauconite grains within this sequence [*Cramer et al.*, 1999]. Our interpretations imply that transgression began ~2m below and the maximum flooding occurred ~1m above the onset of the CIE. Assuming sedimentation rates of between 1 and 10 cm/ka, the transgression initiated ~20–200 ka before the CIE and continued for ~10 ka after the onset of the CIE. Importantly, the coastline migrated farther away from the site during the PETM, even though sediment supply to the New Jersey Shelf increased tremendously [*Sluijs et al.*, 2007b; *John et al.*, 2008].

[26] A sea level fall during the upper part of the CIE is suggested by higher BIT values, but not by variations in dinocyst assemblages or the amount of coarse sediment. However, a sequence boundary clearly truncates the upper bound of the PETM at ~347 mbs [*Cramer et al.*, 1999]. Sediments overlying this sequence boundary accumulated during a younger transgression, as they occur within Chron C24n [*Cramer et al.*, 1999] and contain dinocysts, such as the genus *Wetzeliella*, that originated close to ETM2 [*Heilmann-Clausen*, 1985; *Powell et al.*, 1996; *Bujak and Brinkhuis*, 1998].

[27] Near the base of the Wilson Lake section (Figure 4), the S/A index increases while % lagoonal taxa, wt. % sand and BIT values decrease. We again interpret these changes as signifying a transgression. This transgression begins ~1.5 m below the onset of the CIE, although the step in carbon isotope composition is less defined at Wilson Lake than at Bass River (Figure 4). We infer the mfs to correspond to the maximum in S/A index, and minima in wt. % sand and BIT index, which are found ~80 cm above the onset of the CIE (Figure 4). Assuming sedimentation rates of 1 to 8.4 cm/ka immediately before and during the PETM [*Gibbs et al.*, 2006], the transgression again started ~20–200 ka before the CIE, and maximum flooding again occurred ~10 ka after the onset of the CIE. The overall pattern of sea level change at Wilson Lake, hence, mimics that recorded at Bass River, with the shoreline migrating inland even as the sediment supply increased.

[28] In the Wilson Lake section, a sequence boundary is noted at ~96.5 mbs. Similar to Bass River, sediments overlying this sequence boundary mark a younger transgression and contain the dinocyst genus *Wetzeliella*, indicating an upper Chron C24r or Chron C24n age [*Heilmann-Clausen*, 1985; *Powell et al.*, 1996; *Bujak and Brinkhuis*, 1998], consistent with previous age assessments [*Gibbs et al.*, 2006].

5.1.2. Woensdrecht, Southeastern North Sea

[29] Upper Paleocene-lower Eocene strata in the Woensdrecht borehole (Figure 5a) can be dated using available dinocyst biostratigraphy [*Munsterman*, 2004] and the dinocyst biostratigraphic framework for the North Sea [e.g., *Bujak and Mudge*, 1994; *Powell et al.*, 1996]. Sediment between ~650–626 mbs was deposited during the late Paleocene *Alisocysta margarita* Zone [*Powell*, 1992], as *A. margarita* is consistently present and *Areoligera gippingensis* abundant. Moreover, the LO of *A. gippingensis* at 626 mbs corresponds to upper Nannofossil Zone NP6 (early Thanetian at ~58 Ma) throughout the North Sea [*Bujak and Mudge*, 1994; *Powell et al.*, 1996]. However, sediments between ~624 and 610 mbs contain abundant *Apectodinium* spp., including *A. augustum*, which characterize the PETM in many Northern Hemisphere sections [*Bujak and Brinkhuis*, 1998; *Steurbaut et al.*, 2003; *Sluijs*, 2006]. Hence, these sediments were deposited during the PETM, an interpretation corroborated by a ~5‰ negative step in $\delta^{13}C_{TOC}$ from −23‰ to −28‰ at ~624 mbs (Figure 5a). A sandstone unit between 609–604 mbs does not contain palynomorphs, but dinocyst assemblages just above are also dominated by *Apectodinium*. *A. augustum* is not found, and the $\delta^{13}C_{TOC}$ of ~25‰ is much higher than for the PETM, indicating that this interval was deposited after the PETM. At ~595 mbs,

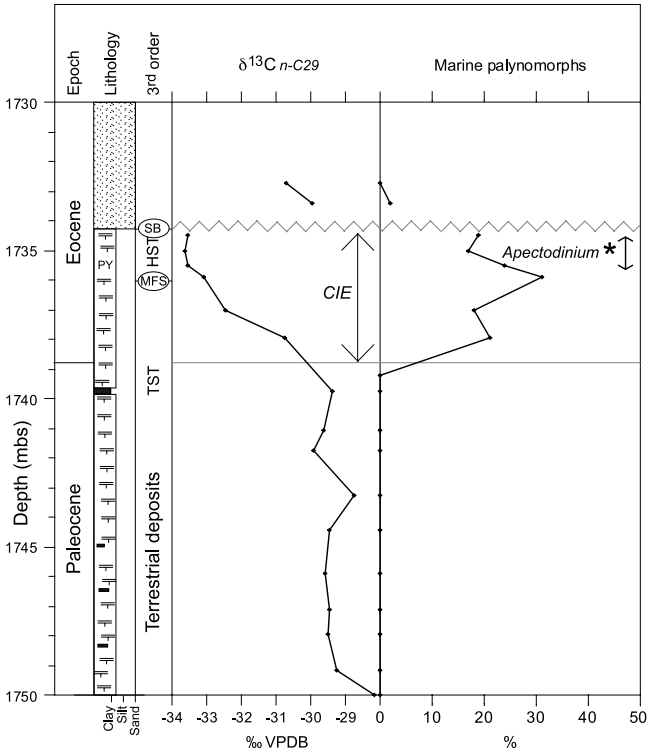

Figure 6. Kumaru, New Zealand: lithology, C29 n-alkane ($\delta^{13}C_{n\text{-}C29}$), and percentage marine palynomorphs across the PETM. Asterisk indicates >30% of the dinocyst assemblage.

taxa such as *Wetzeliella articulata*, *W. meckelfeldensis*, *Dracodinium pachydermum* and *D. varielongitudum* are recorded; these taxa originated at least 1.5 Ma after the PETM [*Powell et al.*, 1996; *Bujak and Brinkhuis*, 1998]. Given this timing, it is possible that the ~1‰ negative step at 604 mbs (Figure 5a) along with abundant *Apectodinium*, indicates ETM2 or the X-event, although further age constraints are required to confirm which one, if either, is present in the section.

[30] The unconformities between sedimentary units in the Woensdrecht section preclude accurate sedimentation rate calculations. Nevertheless, a basic depositional history can be reconstructed. Sediment was deposited in shallow marine water during the early Thanetian and again during the PETM (Figure 5a). The ~2.5 Ma intervening hiatus represents a time of nondeposition or erosion, probably during a phase of low sea level. Thus, sedimentation at this site resumed during the PETM. The overall sequence stratigraphy appears similar to that of the adjacent section at Doel [*Steurbaut et al.*, 2003] (see below (Figure 5b)). Similar to the New Jersey sites, the upper bound of the PETM at Woensdrecht is truncated by a sandstone unit that marks a sequence boundary (Figure 5a). This may represent the transgressive sands of the subsequent transgression, which, according to the age model, occurred at least 1.5 Ma after the PETM, perhaps at the time of ETM2 or the X-event.

5.1.3. Kumara-2

[31] Palynomorph assemblages from the Kumara-2 cores are well preserved and diverse throughout the interval examined, apart from a ~10m interval of coarse channel fill sands between 1734 and 1724 mbs (Figure 6). Generally, sediment samples only contain terrestrial palynomorphs, implying deposition on land. Between ~1738 and ~1733.5 mbs, however, marine dinocysts compose up to 31% of the total palynomorph assemblage (Figure 6). Up to 54% of the dinocyst assemblage are *Apectodinium* [*Kennedy et al.*, 2006], although not *A. augustum*, which in the Southern Hemisphere has only been reported from offshore Brazil [*Ferreira et al.*, 2006]. Other dinocyst taxa include *Spiniferites, Fibrocysta, Operculodinium* and *Kenleyia*. Moreover, pollen of angiosperm taxa associated with thermophilic conditions, such as *Cupanieidites orthoteichus* and *Spinizonocolpites prominatus*, appear at ~1738 mbs [*Crouch et al.*, 2005].

[32] Pollen of thermophilic angiosperm taxa (e.g., *Cupanieidites orthoteichus* and *Spinizonocolpites prominatus*) first occur at ~1738 mbs [*Crouch et al.*, 2005]. These occurrences are regionally correlated to the base of the New Zealand Waipawan Stage [*Raine*, 1984; *Morgans et al.*, 2004], equivalent to the base of the Eocene [*Hancock et al.*, 2003]. With the present sample resolution, the beginning of marine sediments corresponds to a ~4‰ negative shift in the $\delta^{13}C_{n\text{-}C29}$, which we ascribe to the CIE (Figure 6).

[33] The CIE spans a ~6–7 m interval (~1739 to 1732.5 m) of marine sediment, which indicates transgression during the PETM (Figure 6). The termination the CIE is a sharp return to near preexcursion values and coincides with the uppermost occurrence of marine sediments. This culmination suggests that the upper part of the CIE is missing and precludes good estimates of sedimentation rates. With the current resolution, we cannot state whether the transgression was concomitant with the CIE. Nevertheless, on the basis of the peak abundance of marine palynomorphs, we place the MFS just below the most negative $\delta^{13}C$ values of the PETM.

5.2. Comparable Records at Other Marginal Marine Locations

5.2.1. Doel, Southeastern North Sea

[34] Early Paleogene sections have been cored at Doel and Kallo, Belgium. The sections were deposited ~15–20 km south of the Woendrecht section, and thereby closer to the paleo-shoreline [*Steurbaut et al.*, 2003]. The two sequences are very similar [*Steurbaut et al.*, 2003], and for brevity we only discuss the one at Doel (Figure 5b).

[35] Sediments between 473 and 470 mbs represent the Grandglise Sand Member, which has been dated as early Thanetian (~58 Ma), on the basis of the presence of nannofossil taxa *Heliolithus riedelii* and *Hornibrookina arca* (NP8) and the recognition of the *Alisocysta margarita* dinocyst Zone [*Steurbaut*, 1998]. An erosive surface is present at 473 mbs [*Steurbaut*, 1998]. Sediments above this surface, composed of clay and silt, were deposited during the PETM, on the basis of the presence of *Apectodinium augustum* and a ~5‰ negative CIE in $\delta^{13}C_{TOC}$ [*Steurbaut et al.*, 2003] (Figure 5b). Similar to the cores from Woendrecht, this implies a ~2.5 Ma hiatus below the PETM. The remainder of the section has poor age control, apart from the termination of the PETM; at ~453 mbs, there is a ~1.5‰

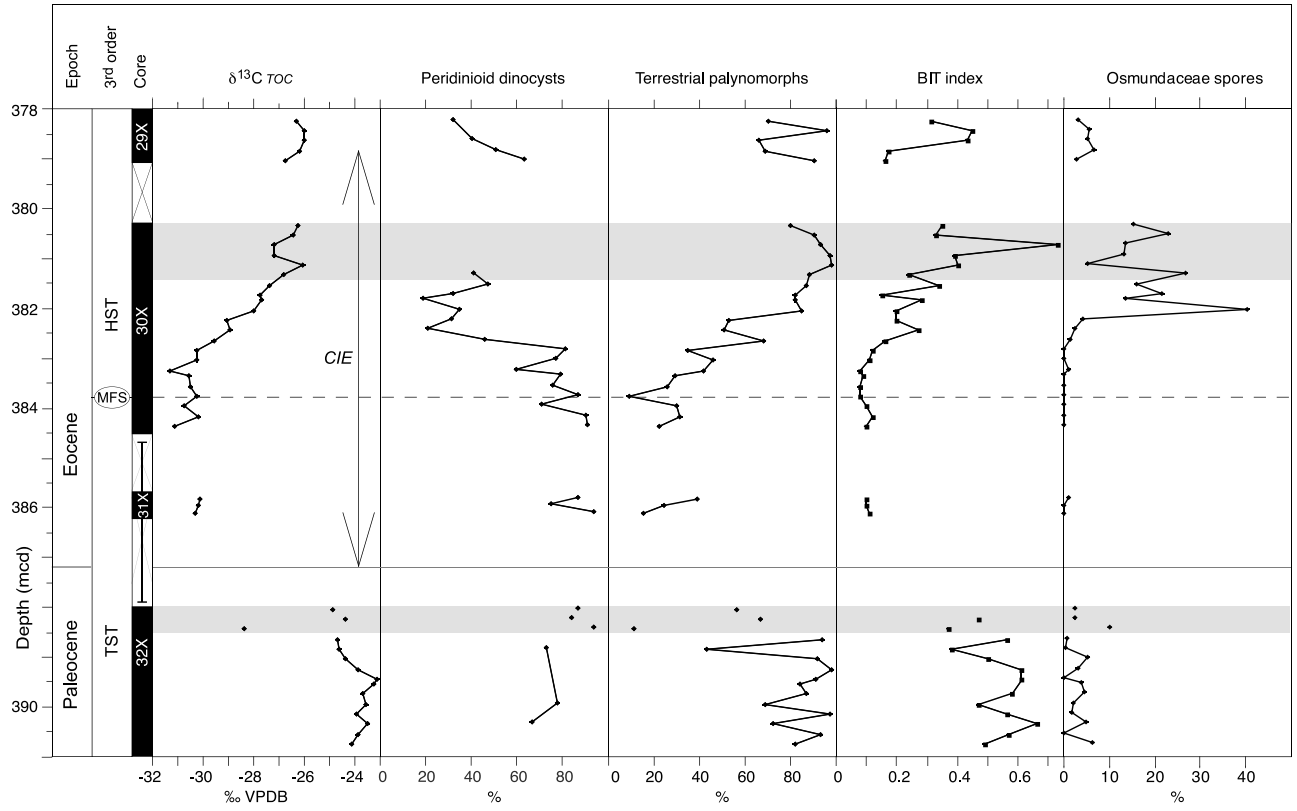

Figure 7. Lomonosov Ridge, Arctic Ocean: sequence stratigraphic interpretation, TOC $\delta^{13}C$, percentage terrestrial palynomorphs, and BIT index data (all from *Sluijs et al.* [2006]), and percentage peridinioid dinocysts and percent Osmundaceae spores [from *Sluijs et al.*, 2008], through the latest Paleocene-earliest Eocene. mcd, meters composite depth.

positive step in $\delta^{13}C_{TOC}$, which coincides with the LO of *A. augustum*. The first occurrence of *Wetzeliella astra* at ~443 mbs [*Steurbaut et al.*, 2003] suggests an age at least 1.5 Ma younger than the PETM.

[36] Similar sequences, with a hiatus between the early Thanetian and the PETM, have been recognized in sections along southeastern Great Britain [*Powell et al.*, 1996; *Bujak and Brinkhuis*, 1998; *Payne et al.*, 2005]. The uppermost Paleocene hiatus would be difficult to explain by reduced sediment supply at all these sites. More likely, it represents erosion during relatively low sea level. This is supported by the erosive surface that typifies the top of the Grandglise Sand Member in the Dutch and Belgian sections [*Steurbaut*, 1998]. The resumption of marine sedimentation during the PETM, therefore, suggests a marine incursion.

5.2.2. Lomonosov Ridge, Central Arctic Ocean

[37] Uppermost Paleocene-lowermost Eocene sediments on Lomonosov Ridge were deposited on the shelf close to land, as indicated by high abundances of terrestrial components, including plant remains and large spores [*Backman et al.*, 2006; *Sluijs et al.*, 2006, 2008]. Cenozoic marine sedimentation at this site commenced at least 1 Ma prior to the PETM [*Backman et al.*, 2006]. The PETM was identified on the basis of the CIE in $\delta^{13}C_{TOC}$ and the occurrence of *A. augustum* [*Sluijs et al.*, 2006].

[38] Dinocyst assemblages through the PETM are dominated by Peridinioid taxa (Figure 7), which reflect low salinities and eutrophic conditions [*Sluijs et al.*, 2006, 2008]. In fact, salinities in the Arctic Ocean appear to have been sufficiently low during the PETM that Gonyaulacoid taxa, such as *Spiniferites* and *Areoligera*, are quite rare [*Sluijs et al.*, 2008]. For this reason, variations in proximity to the coast are difficult to extract from dinocyst assemblages.

[39] Late Paleocene through earliest Eocene palynological assemblages at Lomonosov Ridge often yield >90% terrestrial palynomorphs (spores and pollen). However, during the PETM, the relative abundance of terrestrial palynomorphs drops (Figure 7) [*Sluijs et al.*, 2006]. The abundance of Taxodiaceae pollen and Osmundaceae spores also declines [*Sluijs et al.*, 2006, 2008] (Figure 7). These relatively large palynomorphs do not disperse easily. Their absence in sediments across the PETM suggests that the site was then located far from shore. Additionally, BIT values drop and Rock Eval Hydrogen Index rises across the PETM [*Sluijs et al.*, 2006]. This also suggests a decline in the relative amount of terrestrial organic matter because of a greater distance from shore [*Sluijs et al.*, 2006]. One might suggest a decrease in river inputs and the supply of terrestrial material. However, organic geochemical and dinocyst assemblage evidence point to decreased salinity, enhanced surface water stratification, and elevated siliciclastic sedi-

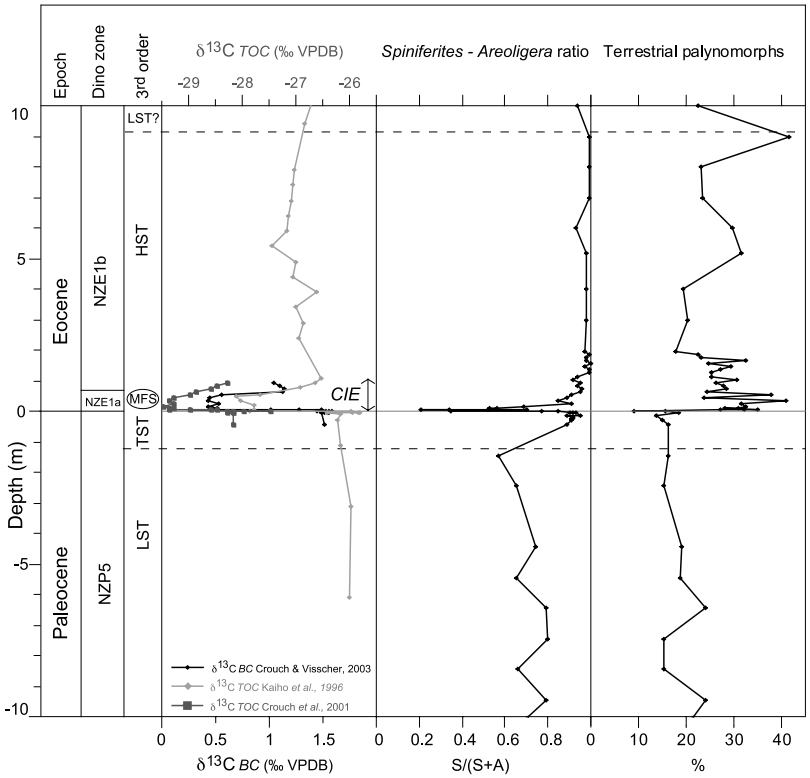

Figure 8. Tawanui, New Zealand; sequence stratigraphic interpretation, BC [from *Crouch and Visscher*, 2003], TOC $\delta^{13}C$ [from *Kaiho et al.*, 1996; *Crouch et al.*, 2001], percentage terrestrial palynomorphs [from *Crouch et al.*, 2003b], and *Spiniferites*/*Areoligera* ratio (calculated from data in the paper by *Crouch and Brinkhuis* [2005]) through the latest Paleocene-earliest Eocene.

ment supply in the central Arctic Ocean during the PETM [*Sluijs et al.*, 2006, 2008].

5.2.3. Tawanui, New Zealand

[40] An upper Paleocene to lower Eocene section is exposed along Tawanui River in the North Island [*Kaiho et al.*, 1996] (Figure 8). The section was deposited on a continental slope in upper middle bathyal water depths based on benthic foraminifer assemblages [*Kaiho et al.*, 1996]. However, high abundances of terrestrial components indicate the site must have been proximal to the coastline [*Kaiho et al.*, 1996; *Crouch et al.*, 2003b]. The Tawanui section yields rich palynological assemblages, which include marine and terrestrial palynomorphs [*Crouch et al.*, 2003b; *Crouch and Brinkhuis*, 2005]. Dinocysts characteristic of neritic settings are present, but these were likely transported off the shelf [*Crouch et al.*, 2003b].

[41] The PETM is marked by a prominent CIE in multiple carbon-bearing phases [*Kaiho et al.*, 1996; *Crouch et al.*, 2001; *Crouch and Visscher*, 2003] (Figure 8). This interval has a significant increase in the amounts of terrestrial palynomorphs, terrestrial organic carbon, and terrigenous minerals [*Crouch et al.*, 2001, 2003b]. These patterns suggest increased delivery of continental material during the PETM, similar to inferences made elsewhere (Figure 2). Nonetheless, a rise in sea level is also indicated, on the basis of increased abundances of the open marine members of the dinocyst genus *Operculodinium* spp. [*Crouch and Brinkhuis*, 2005]. A high in the S/A index across the PETM (Figure 8) further supports a sea level rise, because it implies that the source of *Areoligera* cpx moved away from the site.

[42] One could argue that the transient decrease in the S/A index just above the onset of the CIE reflects sea level lowering. However, this interval represents a glauconite-rich layer that represents redeposited shelf material [*Kaiho et al.*, 1996]. The decrease in S/A index is consistent with that interpretation.

5.3. Eustatic Rise During the Paleocene-Eocene Thermal Maximum

[43] Palynological and organic biomarker records indicate that the coastline moved landward from multiple marine locations across the globe during the PETM. At several of these sites, this transgression occurred despite increasing sediment supply from the continents, which would normally lead to basin fill and relative sea level fall. Collectively, the evidence points to a eustatic rise, which at least in the New Jersey sections initiated prior to the CIE and has its MFS within the CIE (Figure 9). The sea level rise corresponds to a package of sediment (sequence) called Paleocene-3 (Pa-3) on the New Jersey Shelf [*Liu et al.*, 1997; *Miller et al.*, 1998a] and named Thanetian-5 (Tht-5) in the North Sea [*Hardenbol*, 1994; *Powell et al.*, 1996; *Bujak and Brinkhuis*, 1998; *Payne et al.*, 2005].

[44] Further evidence supporting a eustatic rise across the PETM comes from microfossil studies at several other locations. In continental margin sections in California, United States, a decrease in grain size across the onset of the PETM is consistent with sea level rise [*John et al.*, 2008]. In northern Egypt, ostracode assemblages show increased abundances of upper bathyal and outer neritic taxa from the upper Paleocene to lower Eocene consistent with a ~20 m rise in sea level [*Speijer and Morsi*, 2002] (Figure 9). In other Tethyan margin sequences, benthic foraminifer assemblages and lithological evidence also indicate transgression during the PETM [*Speijer and Schmitz*, 1998; *Speijer and Wagner*, 2002; *Gavrilov et al.*, 2003]. Uppermost Paleocene sediments in the Sokolovsky Quarry section in the Turgay Strait, Kazakhstan, contain abundant *Areoligera*, with one exception, the PETM (identified on the basis of *A. augustum*), which contains the highest abundances of offshore dinocysts consistent with transgression [*Iakovleva et al.*, 2001] (Figure 9). This interpretation is supported by the influx of open marine diatoms during the PETM, while uppermost Paleocene assemblages were dominated by shallow water taxa [*Radionova et al.*, 2001; *Oreshkina and Oberhänsli*, 2003].

[45] Some authors have suggested a drop in sea level across the PETM on the basis of increased sedimentation rates in sequences in northern Spain, which were interpreted to reflect enhanced hinterland erosion due to an increase in topographic relief resulting from regression [*Schmitz and Pujalte*, 2003]. More recent studies, however, have attributed increased erosion rates in this basin to an intensification of seasonal precipitation during the PETM [*Schmitz and Pujalte*, 2007]. On the basis of a recent revision of the stratigraphy of the sediments, regression was redated as latest Paleocene, followed by transgression during the PETM [*Pujalte and Schmitz*, 2006]. Regression close to the PETM interval has also been recorded in the Norwegian-Greenland Sea and northern North Sea, which has been explained by tectonic-forced uplift, related to the North Atlantic igneous province [e.g., *Maclennan and Jones*, 2006].

5.4. Other Eustatic Fluctuations During the Latest Paleocene and Early Eocene

[46] The compiled records also reveal distinct sea level fluctuations prior to and after the PETM. One or more of the highs might be associated with other hyperthermals, particularly ETM2 or the so-called X-event.

5.4.1. Latest Paleocene

[47] At Bass River, we tentatively identified an interval of maximum flooding during Chron C25n ca. 57.2−56.5 Ma (Figure 3). This likely corresponds to a highstand sequence found across New Jersey and referred to as pa-2 [*Liu et al.*, 1997]. This sequence, in turn, may correlate with highstand sequences in the North Sea (Thanetian 4) [*Powell et al.*, 1996] and the Turgay Strait [*Iakovleva et al.*, 2001], although the chronostratigraphy in these regions remain poorly constrained [*Powell et al.*, 1996; *Bujak and Brinkhuis*, 1998; *Payne et al.*, 2005] (Figure 9). Nevertheless, this transgression appears to have been global in nature, thus representing a eustatic rise.

5.4.2. Early Eocene Hyperthermals

[48] At the neritic sites of New Jersey, the North Sea and the Turgay Strait, the upper part of the PETM is truncated in a sequence boundary, marking a post-PETM regression (Figure 9). Sediments overlying this sequence boundary fall within the uppermost part of Chron C24r or lowermost C24n (~53 Ma), indicating a 1.5−2 Ma hiatus between the PETM and the overlying unit. In New Jersey, these sediments mark the next transgression and compose sequence E1 [*Browning et al.*, 1996; *Miller et al.*, 1998a] (Figure 9). Correlation to sequences from the UK margin is complicated, but it should correspond to either Ypresian-2 (Ypr-2), or the classic London Clay Transgression sequence Ypr-3 [*Powell et al.*, 1996; *Bujak and Brinkhuis*, 1998; *Miller et al.*, 2005b; *Payne et al.*, 2005]. Although the timing of this MFS is not well constrained, it may correspond to ETM2 or the X-event, given the high abundances of *Apectodinium* spp. and a small negative carbon isotope excursion in the Woensdrecht section at that level (Figure 5).

5.5. Mechanisms of Eustatic Variation

5.5.1. Glacioeustacy

[49] Discussion exists on whether the late Paleocene and early Eocene greenhouse world had continental ice sheets of a size that would be significant for glacioeustasy [e.g., *Zachos et al.*, 2001; *DeConto and Pollard*, 2003; *Miller et al.*, 2005b]. Using a coupled climate and ice sheet model, *DeConto and Pollard* [2003] assess the sensitivity of Antarctic ice sheets in the Eocene to varying atmospheric CO_2 concentrations. They conclude that ice sheets with mass sufficient to drive 10 m of sea level change could have existed in alpine Antarctic regions during the latest Paleocene-earliest Eocene under certain orbital configuration. This scale of glacioeustacy, which is consistent with inferences based on observations [*Miller et al.*, 2005b], might have been (partly) sufficient to drive the recorded sea level cycles.

[50] The potential contribution to sea level change from these ice sheets would have been dependent on the orbital parameters, particularly obliquity, which through sea level

Figure 9. Compilation of latest Paleocene and earliest Eocene sequence stratigraphies. An age of 55.5 Ma is assumed for the onset of the PETM, and subsequently the ages of magnetochron reversals associated with C25n and the onset of C24n.3n were calculated using the durations of *Westerhold et al.* [2007]. Durations of Chrons C24n.3n, C24n.2n, and C24n.1n are from *Ogg and Smith* [2004]. Question marks indicate sequences of which precise dating is uncertain, and gray crosses indicate hiatuses. Study 1, this study; study 2 after *Powell et al.* [1996] and *Bujak and Brinkhuis* [1998]; study 3, after *Payne et al.* [2005]; study 4, after *Iakovleva et al.* [2001]; study 5, after *John et al.* [2008]; study 6, after *Speijer and Morsi* [2002]; and study 7, after *Crouch and Brinkhuis* [2005]. $LST_{(2)}$, Lowstand Systems Tract Type 2.

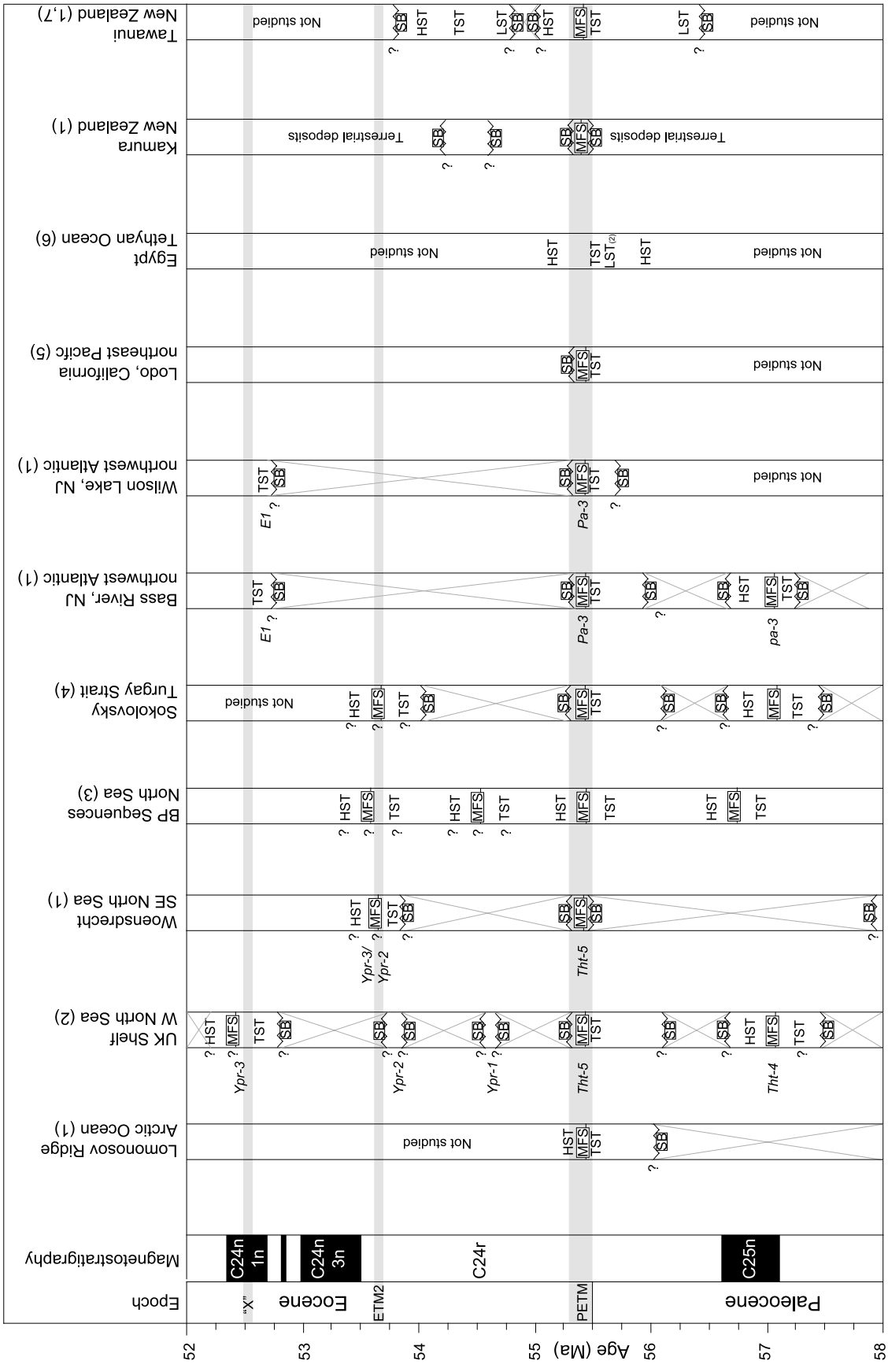
Age (Ma)
52
53
54
55
56
57
58
Epoch
Magnetostratigraphy
Lomonosov Ridge Arctic Ocean (1)
UK Shelf W North Sea (2)
Woensdrecht SE North Sea (1)
BP Sequences North Sea (3)
Sokolovsky Turgay Strait (4)
Bass River, NJ northwest Atlantic (1)
Wilson Lake, NJ northwest Atlantic (1)
Lodo, California northeast Pacific (5)
Egypt Tethyan Ocean (6)
Kamura New Zealand (1)
Tawanui New Zealand (1,7)
"X"
Eocene
Paleocene
C24n 1n
C24n 3n
C24r
C25n
ETM2
PETM
Not studied
Terrestrial deposits
HST
TST
MFS
SB
LST
LST(2)
Ypr-3
Ypr-2
Ypr-1
Tht-5
Tht-4
E1
Pa-3
pa-3

Figure 9

should be expressed globally [*DeConto and Pollard*, 2003]. Obliquity related cycles, however, are either relatively weak (compared to precession) or absent in upper Paleocene and lower Eocene marine records [e.g., *Röhl et al.*, 2003; *Lourens et al.*, 2005; *Westerhold et al.*, 2007; *Sluijs et al.*, 2008], questioning the existence of the hypothesized ice sheets and their contribution to sea level changes.

5.5.2. Steric Effect

[51] For the long-term late Paleocene-early Eocene warming trend, and particularly for the PETM and other hyperthermals, another mechanism of sea level rise is thermal expansion of ocean water. The temperature-density relationship of seawater (1.9×10^{-2} %volume/°C) requires a 3–5 m rise in sea level from the ~5°C ocean warming recorded during the PETM [*Kennett and Stott*, 1991; *Zachos et al.*, 1993; *Thomas and Shackleton*, 1996; *Thomas et al.*, 2002; *Zachos et al.*, 2003; *Tripati and Elderfield*, 2005; *Sluijs et al.*, 2006; *Zachos et al.*, 2006]. Our most expanded records from New Jersey indeed show a reasonable correlation between sea level rise and local PETM surface warming (likely synchronous with deep ocean warming on timescales of 1 or a few thousand years) (Figures 3 and 4). However, although locally at Bass River the onset of SST rise appears to coincide roughly with sea level rise, the sea level rise started prior to PETM-related global warming. This trend could have been influenced by regional factors such as variations in sediment supply but if global, the early onset of eustatic rise implies contribution from another mechanism.

5.5.3. Tectonic/Volcanic Forcing

[52] The establishment of the North Atlantic Igneous Province (NAIP) produced large amounts of young crust, increased the length of the midocean ridge and probably elevated the ocean floor [*Roberts et al.*, 1984; *White and McKenzie*, 1989; *Eldholm and Grue*, 1994; *Saunders et al.*, 1997; *Holbrook et al.*, 2001] and may have contributed to sea level rise. The NAIP was not included in the recent reconstruction of ocean basin volume by *Müller et al.* [2008], indicating that the estimated volume for this time interval could be too high, resulting in underestimates of sea level. Some of the NAIP volcanism was submarine, judging from the occurrence of marine dinocysts in sediments that locally alternate with the basalts [e.g., *Boulter and Manum*, 1989], and may have affected sea level on million-year scale by decreasing the ocean basin volume. Along with uncertainties in the long-term subsidence history of the New Jersey margin due to the previously neglected influence of the subducting Farralon slab [*Müller et al.*, 2008], this may explain part of the large discrepancy between the *Kominz et al.* [2008] backstripping estimates and the record of *Müller et al.* [2008]. Part of the NAIP volcanism was subaerial, thereby injecting CO_2 into the atmosphere that perhaps caused long-term ocean warming of several degrees (Figure 1) [*Thomas and Bralower*, 2005], and associated thermal expansion of the ocean by several meters.

[53] Rapid submarine uplift during the establishment of the NAIP close to the PETM [*Maclennan and Jones*, 2006] could have decreased the volume of the ocean basins on somewhat shorter timescales. Such processes may increase sea level by up to 5 m [*Müller et al.*, 2008] and could have contributed to eustatic rise during the PETM if they were coeval [*Storey et al.*, 2007].

5.5.4. Summary

[54] Despite recent progress, reconstruction of late Paleocene-early Eocene spreading rates and ocean basin volume is as yet insufficient to reconstruct its effect on long-term late Paleocene-early Eocene sea level, since the NAIP is not yet incorporated in the calculations [*Müller et al.*, 2008]. The mismatch (Figure 1) in absolute sea level of up to 70 m between estimates derived from backstripping [*Kominz et al.*, 2008] and basin volume [*Müller et al.*, 2008] could, partly, be attributed to reduced ocean basin volume. Alternatively, long-term subsidence of New Jersey is still underestimated [*Müller et al.*, 2008]. If the *Kominz et al.* [2008] record is correct, the mismatch between peak temperatures and peak sea level (Figure 1) suggests that long-term ocean warming [*Zachos et al.*, 2001] and associated steric effects was not a dominant factor in determining long-term sea level sea level. Rather, it would imply that long-term ocean volume was not constant through this interval.

[55] On shorter timescales, such as the PETM, uncertainties related to New Jersey subsidence on tectonic timescales should not have influence the sea level interpretations. Uplift of oceanic crust during the establishment of the NAIP may have contributed several meters of sea level rise. If variations in ice volume drove the recorded sea level variations and if the ice volume estimates of *DeConto and Pollard* [2003] and *Miller et al.* [2005b] are correct, third-order sea level changes during the late Paleocene and the early Eocene, including the one at the PETM, were less than ~20 m, and likely less than 10 m. In addition to ice volume influences, thermal expansion must have contributed up to 5 m to eustacy. The above mechanisms would conspire to raise global sea level by up to 20–30 m at the time of the PETM. If the MFS we locally recognize within Chron C25n will appear to be global, this was likely tectonically forced because no evidence for rapid global warming has, as yet, been documented for this time period. In our most expanded records of the onset of the PETM in New Jersey the rise in sea level preceded the onset of warming (Figures 3 and 4). This suggests that early sea level rise was forced by tectonism, followed by steric effects and potential ice sheet melting during the PETM warming, to contribute to the globally recognized MFS during the PETM (Figure 9).

5.6. Implications for Triggering Hyperthermal Events

[56] The source of ^{13}C-depleted carbon at the initiation of the PETM remains an outstanding problem. To date, several mechanisms have been proposed (see overview in the paper by *Sluijs et al.* [2007a]). Two require a drop in sea level over extensive regions. In theory, a major sea level fall could have released large amounts of microbially derived methane stored in pore waters of sediments on the shelf or slope [*Schmitz et al.*, 2004]. Our results show eustatic rise during the PETM, refuting the hypothesis that sea level lowering caused methane injection.

[57] Second, isolation of large epicontinental seaways, followed by desiccation and oxidation of organic matter, might also have added large amounts of CO_2 to the atmosphere during the PETM [*Higgins and Schrag*,

2006]. The primary epicontinental sea underlying this hypothesis is located in Eurasia, representing the Turgay Strait, Southeastern Europe and South Asia. However, desiccation of this area is inconsistent with the recorded sea level rise. Indeed, expanded marine deposits that record transgression have been documented from the PETM of these regions [*Iakovleva et al.*, 2001; *Radionova et al.*, 2001; *Crouch et al.*, 2003a; *Oreshkina and Oberhänsli*, 2003; *Akhmetiev and Beniamovski*, 2004] (Figure 9).

6. Conclusions

[58] Palynological, lithological and organic biomarker records show that widely separated sections from the Arctic Ocean, New Jersey Shelf, Western United States, North Sea, Russia, the southern Tethyan margin and New Zealand became located further from the coast during the PETM. At several of these sites, this transgression occurred despite increasing sediment supply from the continents, which would normally cause relative sea level fall because of basin fill. Collectively, the evidence points to eustatic rise. The sites from New Jersey indicate that significant sea level rise began 20–200 ka before the CIE, while an MFS is identified within the PETM on a global scale. Hypotheses for the cause of the PETM that require a sea level drop can therefore be refuted. The records from New Jersey, North Sea and epicontinental Russia suggest that sea level rose again during Chron C24n. This phase is close to the onset of the EECO, ETM2 (~53.5 Ma) and the X-event (~52 Ma), suggesting a relation between phases of extreme global warmth and sea level change.

[59] Several meters of transgression during the PETM and potentially the other hyperthermals can be attributed to thermal expansion of seawater as a result of ocean warming. If small ice sheets persisted on Antarctica during the late Paleocene and early Eocene, these would have likely melted during the hyperthermals, potentially contributing an additional 10m to sea level rise. Interestingly, the onset of sea level rise appears, at least regionally to have preceded the PETM. Hence, perhaps tectonic uplift of ocean floors in the North Atlantic Igneous Province contributed to sea level rise.

[60] **Acknowledgments.** This research used samples and/or data provided by the Integrated Ocean Drilling Program (IODP). Appy Sluijs thanks the Utrecht Center of Biogeology, the LPP Foundation, Utrecht University, and the Netherlands Organisation for Scientific Research (NWO; VENI grant 863.07.001) for funding. This research was supported by NSF grant EAR-0628719 to Zachos. Richard Pancost and Luke Handley acknowledge support from the NERC for funding Handley's Ph.D. studentship. Appy Sluijs, Henk Brinkhuis, Dirk Munsterman, Gert-Jan Reichart, Stefan Schouten, Jaap Sinninghe Damsté, Natasja Welters, and André Lotter thank NWO for their continued support of the IODP. We thank Debbie Thomas and an anonymous reviewer for constructive reviews and James Browning, Ben Cramer, Matt Huber, Luc Lourens, Ken Miller, Dietmar Müller, and Michelle Kominz for discussions.

References

Abdul Aziz, H., F. J. Hilgen, G. M. van Luijk, A. Sluijs, M. J. Kraus, J. M. Pares, and P. D. Gingerich (2008), Astronomical climate control on paleosol stacking patterns in the upper Paleocene-lower Eocene Willwood Formation, Bighorn Basin, Wyoming, *Geology*, *36*, 531–534, doi:510.1130/G24734A.

Akhmetiev, M. A., and V. A. Beniamovski (2004), Palaeocene and Eocene of Western Eurasia (Russian sector) — Stratigraphy, palaeogeography, climate, *Neues Jahrb. Geol. Palaeontol. Abh.*, *234*, 137–181.

Backman, J., K. Moran, D. B. McInroy, and L. A. Mayer, and The Expedition 302 Scientists (2006), *Proceedings of the Integrated Ocean Drilling Program*, vol. 302, Ocean Drill. Program, College Station, Tex.

Boulter, M. C., and S. B. Manum (1989), The Brito-Arctic igneous province flora around the Paleocene/Eocene boundary, *Proc. Ocean Drill. Program Sci. Results*, *104*, 663–680.

Bowen, G. J., et al. (2006), Eocene hyperthermal event offers insight into greenhouse warming, *Eos Trans. AGU*, *87*(17), doi:10.1029/2006EO170002.

Bradford, M. R., and D. A. Wall (1984), The distribution of recent organic-walled dinoflagellate cysts in the Persian Gulf, Gulf of Oman, and northwestern Arabian Sea, *Palaeontographica*, *192*, 16–84.

Brinkhuis, H. (1994), Late Eocene to early Oligocene dinoflagellate cysts from the Priabonian type-area (northeast Italy); biostratigraphy and palaeoenvironmental interpretation, *Palaeogeogr. Palaeoclimatol. Palaeoecol.*, *107*, 121–163, doi:10.1016/0031-0182(94)90168-6.

Browning, J. V., K. G. Miller, and D. K. Pak (1996), Global implications of lower to middle Eocene sequence boundaries on the New Jersey coastal plain: The icehouse cometh, *Geology*, *24*, 639–642, doi:10.1130/0091-7613(1996)024<0639:GIOLTM>2.3.CO;2.

Bujak, J. P., and H. Brinkhuis (1998), Global warming and dinocyst changes across the Paleocene/Eocene epoch boundary, in *Late Paleocene-Early Eocene Climatic and Biotic Events in the Marine and Terrestrial Records*, edited by M.-P. Aubry, S. G. Lucas, and W. A. Berggren, pp. 277–295, Columbia Univ. Press, New York.

Bujak, J. P., and D. C. Mudge (1994), A high-resolution North Sea Eocene dinocyst zonation, *J. Geol. Soc. London*, *151*, 449–462, doi:10.1144/gsjgs.151.3.0449.

Carter, M., C. Kelly, M. Hillyer, and P. McDowell (1986), Kumara −2, −2A, well completion report, *Pet. Rep. Ser. PR 1183*, 714 pp, Minist. of Econ. Dev., Wellington, N. Z.

Cramer, B. S., M.-P. Aubry, K. G. Miller, R. K. Olsson, J. D. Wright, and D. V. Kent (1999), An exceptional chronologic, isotopic, and clay mineralogic record of the latest Paleocene thermal maximum, Bass River, NJ, ODP 174AX, *Bull. Soc. Geol. Fr.*, *170*, 883–897.

Cramer, B. S., J. D. Wright, D. V. Kent, and M.-P. Aubry (2003), Orbital climate forcing of δ^{13}C excursions in the late Paleocene-early Eocene (chrons C24n–C25n), *Paleoceanography*, *18*(4), 1097, doi:10.1029/2003PA000909.

Crouch, E. M., and H. Brinkhuis (2005), Environmental change across the Paleocene-Eocene transition from eastern New Zealand: A marine palynological approach, *Mar. Micropaleontol.*, *56*, 138–160, doi:10.1016/j.marmicro.2005.05.002.

Crouch, E. M., and H. Visscher (2003), Terrestrial vegetation record across the initial Eocene thermal maximum at the Tawanui marine section, New Zealand, in *Causes and Consequences of Globally Warm Climates in the Early Paleogene*, edited by S. L. Wing et al., *Spec. Pap. Geol. Soc Am.*, 369, 351–363.

Crouch, E. M., C. Heilmann-Clausen, H. Brinkhuis, H. E. G. Morgans, K. M. Rogers, H. Egger, and B. Schmitz (2001), Global dinoflagellate event associated with the late Paleocene thermal maximum, *Geology*, *29*, 315–318, doi:10.1130/0091-7613(2001)029<0315:GDEAWT>2.0.CO;2.

Crouch, E. M., H. Brinkhuis, H. Visscher, T. Adatte, and M.-P. Bolle (2003a), Late Paleocene-early Eocene dinoflagellate cyst records from the Tethys: Further observations on the global distribution of Apectodinium, in *Causes and Consequences of Globally Warm Climates in the Early Paleogene*, edited by S. L. Wing et al., *Spec. Pap. Geol. Soc. Am.*, 369, 113–131.

Crouch, E. M., G. R. Dickens, H. Brinkhuis, M.-P. Aubry, C. J. Hollis, K. M. Rogers, and H. Visscher (2003b), The Apectodinium acme and terrestrial discharge during the Paleocene-Eocene thermal maximum: New palynological, geochemical and calcareous nannoplankton observations at Tawanui, New Zealand, *Palaeogeogr. Palaeoclimatol. Palaeoecol.*, *194*, 387–403, doi:10.1016/S0031-0182(03)00334-1.

Crouch, E. M., J. I. Raine, and E. M. Kennedy (2005), Vegetation and climate change at the Paleocene-Eocene transition, paper presented at Geological Society of New Zealand 50th annual conference, *Geol. Soc. N. Z. Misc. Publ.*, 119A, 1–23.

Dale, B. (1996), Dinoflagellate cyst ecology: Modeling and geological applications, in *Palynology: Principles and Applications*, edited

by J. Jansonius and D. C. McGregor, pp. 1249–1276, Am. Assoc. of Stratigr. Palynologists Found., Dallas, Tex.

DeConto, R. M., and D. Pollard (2003), A coupled climate-ice sheet modeling approach to the early Cenozoic history of the Antarctic ice sheet, *Palaeogeogr. Palaeoclimatol. Palaeoecol.*, *198*, 39–52, doi:10.1016/S0031-0182(03)00393-6.

Dickens, G. R., J. R. O'Neil, D. K. Rea, and R. M. Owen (1995), Dissociation of oceanic methane hydrate as a cause of the carbon isotope excursion at the end of the Paleocene, *Paleoceanography*, *10*, 965–971, doi:10.1029/95PA02087.

Dienst der Rijksopsporing van Delfstoffen (1918), *Eindverslag Over de Onderzoekingen en Uitkomsten van den Dienst der Rijksopsporing van Delfstoffen in Nederland 1903–1916*, Electr. Drukkerij't Kasteel van Aemstel', Amsterdam.

Eldholm, O., and K. Grue (1994), North Atlantic volcanic margins: Dimensions and production rates, *J. Geophys. Res.*, *99*, 2955–2968, doi:10.1029/93JB02879.

Fensome, R. A., and G. L. Williams (2004), The Lentin and Williams index of fossil dinoflagellates 2004, report, 909 pp., Am. Assoc. of Stratigr. Palynologists Found., Houston, Tex.

Fensome, R. A., H. Gocht, and G. L. Williams (1996), *The Eisenack Catalog of Fossil Dinoflagellates*, vol. 4, E. Schweizerbart'sche Verl., Stuttgart, Germany.

Ferreira, E. P., M. C. Viviers, and P. C. Galm (2006), Apectodinium acme in the Paleocene-Eocene transition of the Sergipe Basin, paper presented at Climate and Biota of the Early Paleogene, Univ. of Bilbao, Bilbao, Spain.

Gavrilov, Y., E. A. Shcherbinina, and H. Oberhänsli (2003), Paleocene-Eocene boundary events in the northeastern Peri-Tethys, in *Causes and Consequences of Globally Warm Climates in the Early Paleogene*, edited by S. L. Wing et al., *Spec. Pap. Geol. Soc. Am.*, 369, 147–168.

Gibbs, S. J., T. J. Bralower, P. R. Bown, J. C. Zachos, and L. M. Bybell (2006), Shelf and open-ocean calcareous phytoplankton assemblages across the Paleocene-Eocene Thermal Maximum: Implications for global productivity gradients, *Geology*, *34*, 233–236, doi:10.1130/G22381.1.

Gibson, T. G., L. M. Bybell, and J. P. Owens (1993), Latest Paleocene lithologic and biotic events in neritic deposits of southwestern New Jersey, *Paleoceanography*, *8*, 495–514, doi:10.1029/93PA01367.

Giusberti, L., D. Rio, C. Agnini, J. Backman, E. Fornaciari, F. Tateo, and M. Oddone (2007), Mode and tempo of the Paleocene-Eocene thermal maximum in an expanded section from the Venetian pre-Alps, *Geol. Soc. Am. Bull.*, *119*, 391–412, doi:10.1130/B25994.1.

Hancock, H. J. L., G. R. Dickens, C. P. Strong, C. J. Hollis, and B. D. Field (2003), Foraminiferal and carbon isotope stratigraphy through the Paleocene-Eocene transition at Dee Stream, Marlborough, New Zealand, *N.Z.J. Geol. Geophys.*, *46*, 1–19.

Haq, B. U., J. Hardenbol, and P. R. Vail (1987), Chronology of fluctuating sea levels since the Triassic, *Science*, *235*, 1156–1167, doi:10.1126/science.235.4793.1156.

Hardenbol, J. (1994), Sequence stratigraphic calibration of Paleocene and lower Eocene continental margin deposits in NW Europe and the US Gulf Coast with the oceanic chronostratigraphic record, *Geol. Foeren. Stockholm Foerh.*, *116*, 49–51.

Harland, R. (1973), Dinoflagellate cysts and acritarchs from the Bearpaw Formation (Upper Campanian) of southern Alberta, Canada, *Palaeontology*, *16*, 665–706.

Harland, R. (1983), Distribution maps of recent dinoflagellate in bottom sediments from the North Atlantic Ocean and adjacent seas, *Palaeontology*, *26*, 321–387.

Heilmann-Clausen, C. (1985), Dinoflagellate stratigraphy of the Uppermost Danian to Ypresian in the Viborg 1 borehole, Central Jylland, Denmark, *Aarbog. Dan. Geol. Unders.*, *A7*, 1–69.

Higgins, J. A., and D. P. Schrag (2006), Beyond methane: Towards a theory for the Paleocene-Eocene thermal maximum, *Earth Planet. Sci. Lett.*, *245*, 523–537, doi:10.1016/j.epsl.2006.03.009.

Holbrook, W. S., et al. (2001), Mantle thermal structure and active upwelling during continental breakup in the North Atlantic, *Earth Planet. Sci. Lett.*, *190*, 251–266, doi:10.1016/S0012-821X(01)00392-2.

Hollis, C. J., G. R. Dickens, B. D. Field, C. M. Jones, and C. Percy Strong (2005), The Paleocene-Eocene transition at Mead Stream, New Zealand: A southern Pacific record of early Cenozoic global change, *Palaeogeogr. Palaeoclimatol. Palaeoecol.*, *215*, 313–343, doi:10.1016/j.palaeo.2004.09.011.

Hopmans, E. C., J. W. H. Weijers, E. Schefuß, L. Herfort, J. S. Sinninghe Damsté, and S. Schouten (2004), A novel proxy for terrestrial organic matter in sediments based on branched and isoprenoid tetraether lipids, *Earth Planet. Sci. Lett.*, *224*, 107–116, doi:10.1016/j.epsl.2004.05.012.

Iakovleva, A. I., H. Brinkhuis, and C. Cavagnetto (2001), Late Palaeocene-early Eocene dinoflagellate cysts from the Turgay Strait, Kazakhstan; correlations across ancient seaways, *Palaeogeogr. Palaeoclimatol. Palaeoecol.*, *172*, 243–268, doi:10.1016/S0031-0182(01)00300-5.

John, C. M., S. M. Bohaty, J. C. Zachos, A. Sluijs, S. J. Gibbs, H. Brinkhuis, and T. J. Bralower (2008), North American continental margin records of the Paleocene-Eocene thermal maximum: Implications for global carbon and hydrological cycling, *Paleoceanography*, *23*, PA2217, doi:10.1029/2007PA001465.

Kaiho, K., et al. (1996), Latest Paleocene benthic foraminiferal extinction and environmental change at Tawanui, New Zealand, *Paleoceanography*, *11*, 447–465, doi:10.1029/96PA01021.

Kennedy, E. M., E. M. Crouch, J. I. Raine, L. Handley, and R. D. Pancost (2006), Paleocene-Eocene transition in South Island terrestrial to marginal marine sections, paper presented at Geosciences '06 — Our Planet, Our Future, Geol. Soc. N. Z., Wellington, N. Z.

Kennett, J. P., and L. D. Stott (1991), Abrupt deep-sea warming, palaeoceanographic changes and benthic extinctions at the end of the Palaeocene, *Nature*, *353*, 225–229, doi:10.1038/353225a0.

Kominz, M. A., K. G. Miller, and J. V. Browning (1998), Long-term and short-term global Cenozoic sea-level estimates, *Geology*, *26*, 311–314, doi:10.1130/0091-7613(1998)026<0311:LTASTG>2.3.CO;2.

Kominz, M. A., J. V. Browning, K. G. Miller, P. J. Sugarman, S. Mizintseva, and C. R. Scotese (2008), Late Cretaceous to Miocene sea-level estimates from the New Jersey and Delaware coastal plain coreholes: An error analysis, *Basin Res.*, *20*, 211–226, doi:10.1111/j.1365-2117.2008.00354.x.

Kopp, R. E., T. D. Raub, D. Schumann, H. Vali, A. V. Smirnov, and J. L. Kirschvink (2007), Magnetofossil spike during the Paleocene-Eocene thermal maximum: Ferromagnetic resonance, rock magnetic, and electron microscopy evidence from Ancora, New Jersey, United States, *Paleoceanography*, *22*, PA4103, doi:10.1029/2007PA001473.

Köthe, A. (1990), Paleogene dinoflagellates from Northwest Germany, *Geol. Jahrb.*, *118*, 1–111.

Liu, C., J. V. Browning, K. G. Miller, and R. K. Olsson (1997), Paleocene benthic foraminiferal biofacies and sequence stratigraphy, Island Beach borehole, New Jersey, *Proc. Ocean Drill. Program Sci. Results*, *150X*, 267–375.

Lourens, L. J., A. Sluijs, D. Kroon, J. C. Zachos, E. Thomas, U. Röhl, J. Bowles, and I. Raffi (2005), Astronomical pacing of late Palaeocene to early Eocene global warming events, *Nature*, *435*, 1083–1087, doi:10.1038/nature03814.

Maclennan, J., and S. M. Jones (2006), Regional uplift, gas hydrate dissociation and the origins of the Paleocene-Eocene thermal maximum, *Earth Planet. Sci. Lett.*, *245*, 65–80, doi:10.1016/j.epsl.2006.01.069.

Marret, F., and K. A. F. Zonneveld (2003), Atlas of modern organic-walled dinoflagellate cyst distribution, *Rev. Palaeobot. Palynol.*, *125*, 1–200.

Miller, K. G. (1997), Coastal plain drilling and the New Jersey sea-level transect, *Proc. Ocean Drill. Program Sci. Results*, *150X*, 3–12.

Miller, K. G., R. G. Fairbanks, and G. S. Mountain (1987), Tertiary oxygen isotope synthesis, sea-level history, and continental margin erosion, *Paleoceanography*, *2*, 1–19, doi:10.1029/PA002i001p00001.

Miller, K. G., G. S. Mountain, J. V. Browning, M. Kominz, P. J. Sugerman, N. Christie-Blick, M. E. Katz, and J. D. Wright (1998a), Cenozoic global sea level, sequences, and the New Jersey transect: Results from coastal plain and continental slope drilling, *Rev. Geophys.*, *36*, 569–601, doi:10.1029/98RG01624.

Miller, K. G., et al. (1998b), *Proceedings of the Ocean Drilling Program, Initial Reports*, vol. 174AX, Ocean Drill. Program, College Station, Tex.

Miller, K. G., P. J. Sugarman, J. V. Browning, M. A. Kominz, R. K. Olsson, M. D. Feigenson, and J. C. Hernandez (2004), Upper Cretaceous sequences and sea-level history, New Jersey Coastal Plain, *Geol. Soc. Am. Bull.*, *116*, 368–393, doi:10.1130/B25279.1.

Miller, K. G., M. A. Kominz, J. V. Browning, J. D. Wright, G. S. Mountain, M. E. Katz, P. J. Sugarman, B. S. Cramer, N. Christie-Blick, and S. F. Pekar (2005a), The Phanerozoic record of global sea-level change, *Science*, *310*, 1293–1298, doi:10.1126/science.1116412.

Miller, K. G., J. D. Wright, and J. V. Browning (2005b), Visions of ice sheets in a greenhouse world, *Mar. Geol.*, *217*, 215–231, doi:10.1016/j.margeo.2005.02.007.

Mitchum, R. M., P. R. Vail, and S. Thompson (1977), The depositional sequence as a basic unit for stratigraphic analysis, *Mem. Am. Assoc. Pet. Geol.*, *26*, 53–62.

Morgans, H. E. G., A. G. Beu, R. A. Cooper, E. M. Crouch, C. J. Hollis, C. M. Jones, J. I. Raine, C. P. Strong, G. J. Wilson, and G. S. Wilson (2004), Paleogene (Dannevirke, Arnold and Landon Series), in *The New Zealand Geological Timescale*, vol. 22, edited by R. A. Cooper, chap. 11, pp. 125–163, Inst. of Geol. and Nucl. Sci., Lower Hutt, New Zealand.

Müller, R. D., M. Sdrolias, C. Gaina, B. Steinberger, and C. Heine (2008), Long-term sea-level fluctuations driven by ocean basin dynamics, *Science*, *319*, 1357–1362, doi:10.1126/science.1151540.

Munsterman, D. K. (2004), De resultaten van het dinoflagellaatcysten-onderzoek rondom de Paleoceen-Eoceen grens in boring Raalte (RAL-01), Woensdrecht (WDR-01) en Doel-1B (Belgie), report, 16 pp., Neth. Organ. for Appl. Scientific Res., Utrecht, Netherlands.

Nicolo, M. J., G. R. Dickens, C. J. Hollis, and J. C. Zachos (2007), Multiple early Eocene hyperthermals: Their sedimentary expression on the New Zealand continental margin and in the deep sea, *Geology*, *35*, 699–702, doi:10.1130/G23648A.1.

Ogg, J. G., and A. G. Smith (2004), The geomagnetic polarity time scale, in *A Geologic Time Scale 2004*, edited by F. M. Gradstein et al., Cambridge Univ. Press, Cambridge, UK.

Oreshkina, T. V., and H. Oberhänsli (2003), Diatom turnover in the early Paleogene diatomite of the Sengiley section, middle Povolzhie, Russia: A response to the initial Eocene thermal maximum?, in *Causes and Consequences of Globally Warm Climates in the Early Paleogene*, edited by S. L. Wing et al., *Geol. Soc. Am. Spec. Pap.*, 369, 169–179.

Pancost, R. D., L. Handley, E. Crouch, E. Hankinson, D. Steart, M. Collinson, P. Pearson, and A. Scott (2006), Using higher plant biomarkers to obtain new carbon isotope records across the PETM, paper presented at the General Assembly, Eur. Geosci. Union, Vienna.

Payne, S. N. J., P. A. Cornick, L. F. Draper, H. Nicholson, A. C. Morton, P. Huggins, and R. Anderton (2005), Mungo Field UK North Sea 22/20, 23/16a: Stratigraphy, salt diapirs and reservoir development (or 'The Riddle of the Sands'), in *Recent Developments in Applied Biostratigraphy*, edited by A. J. Powell and J. B. Riding, *Geol. Soc. Spec. Publ.*, 1, 23–42.

Powell, A. J. (1992), Dinoflagellate cysts of the Tertiary System, in *A Stratigraphic Index of Dinoflagellate Cysts, British Micropalaeontological Society Publication Series*, edited by A. J. Powell, pp. 155–251, CRC Press, Boca Raton, Fla.

Powell, A. J., H. Brinkhuis, and J. P. Bujak (1996), Upper Paleocene-lower Eocene dinoflagellate cyst sequence biostratigraphy of southeast England, in *Correlation of the Early Paleogene in Northwest Europe*, edited by R. W. O. B. Knox et al., *Geol. Soc. Spec. Publ.*, 101, 145–183.

Pross, J., and H. Brinkhuis (2005), Organic-walled dinoflagellate cysts as paleoenvironmental indicators in the Paleogene; a synopsis of concepts, *Paläontologische Z.*, *79*, 53–59.

Pujalte, V., and B. Schmitz (2006), Abrupt climatic and sea level changes across the Paleocene-Eocene boundary, as recorded in an ancient coastal plain setting (Pyrenees, Spain), paper presented at Climate and Biota of the Early Paleogene, Univ. of Bilbao, Bilbao, Spain.

Radionova, E. P., I. E. Khokhlova, V. N. Baniamovskii, E. A. Shcherbinina, A. I. Iakovleva, and T. A. Sadchikova (2001), The Paleocene/Eocene transition in the northeastern Peri-Tethys area: Sokolovskii key section of the Turgay Passage (Kazakhstan), *Bull. Soc. Geol. Fr.*, *172*, 245–256, doi:10.2113/172.2.245.

Raine, J. I. (1984), Outline of a palynological zonation of Cretaceous to Paleogene terrestrial sediments in West Coast region, South Island, New Zealand, *Rep. N.Z. Geol. Surv.*, *109*, 1–82.

Reichart, G.-J., H. Brinkhuis, F. Huiskamp, and W. J. Zachariasse (2004), Hyper-stratification following glacial overturning events in the northern Arabian Sea, *Paleoceanography*, *19*, 1, PA2013, doi:10.1029/2003PA000900.

Roberts, D. G., A. C. Morton, and J. Backman (1984), Late Paleocene-Eocene volcanic events in the northern North Atlantic Ocean, *Initial Rep. Deep Sea Drill. Proj.*, *68*, 329–913.

Röhl, U., R. D. Norris, and J. G. Ogg (2003), Cyclostratigraphy of upper Paleocene and lower Eocene sediments at Blake Nose Site 1051 (western North Atlantic), in *Causes and Consequences of Globally Warm Climates in the Early Paleogene*, edited by S. L. Wing et al., *Geol. Soc. Am. Spec. Pap.*, 369, 567–589.

Röhl, U., H. Brinkhuis, C. E. Stickley, M. Fuller, S. A. Schellenberg, G. Wefer, and G. L. Williams (2004), Sea level and astronomically induced environmental changes in middle and late Eocene sediments from the East Tasman Plateau, in *The Cenozoic Southern Ocean: Tectonics, Sedimentation, and Climate Change Between Australia and Antarctica, Geophys. Monogr. Ser.*, vol. 151, edited by N. F. Exon et al., pp. 127–151, AGU, Washington, D. C.

Röhl, U., T. Westerhold, S. Monechi, E. Thomas, J. C. Zachos, and B. Donner (2005), The third and final early Eocene thermal maximum: Characteristics, timing, and mechanisms of the "X" event., paper presented at the Annual Meeting, Geol. Soc. of Am., Salt Lake City, Utah.

Röhl, U., T. Westerhold, T. J. Bralower, and J. C. Zachos (2007), On the duration of the Paleocene-Eocene thermal maximum (PETM), *Geochem. Geophys. Geosyst.*, *8*, Q12002, doi:10.1029/2007GC001784.

Saunders, A. D., J. G. Fitton, A. C. Kerr, M. J. Norry, and R. W. Kent (1997), The North Atlantic Igneous Province, in *Large Igneous Provinces: Continental, Oceanic, and Planetery Flood Volcanism, Geophys. Monogr. Ser.*, vol. 100, edited by J. J. Mahoney and M. F. Coffin, pp. 45–93, AGU, Washington, D. C.

Schmitz, B., and V. Pujalte (2003), Sea-level, humidity, and land-erosion records across the initial Eocene thermal maximum from a continental-marine transect in northern Spain, *Geology*, *31*, 689–692, doi:10.1130/G19527.1.

Schmitz, B., and V. Pujalte (2007), Abrupt increase in seasonal extreme precipitation at the Paleocene-Eocene boundary, *Geology*, *35*, 215–218, doi:10.1130/G23261A.1.

Schmitz, B., V. Pujalte, and K. Nunez-Betelu (2001), Climate and sea-level perturbations during the Initial Eocene Thermal Maximum: Evidence from siliciclastic units in the Basque Basin (Ermua, Zumaia and Trabakua Pass), northern Spain, *Palaeogeogr. Palaeoclimatol. Palaeoecol.*, *165*, 299–320, doi:10.1016/S0031-0182(00)00167-X.

Schmitz, B., B. Peucker-Ehrenbrink, C. Heilmann-Clausen, G. Åberg, F. Asaro, and C.-T. A. Lee (2004), Basaltic explosive volcanism, but no comet impact, at the Paleocene-Eocene boundary: High-resolution chemical and isotopic records from Egypt, Spain and Denmark, *Earth Planet. Sci. Lett.*, *225*, 1–17, doi:10.1016/j.epsl.2004.06.017.

Scotese, C. P., and J. Golanka (1992), *Paleogeographic atlas*, PALEOMAP Prog. Rep. 20-0692, 34 pp., Univ. of Tex., Arlington, Tex.

Sluijs, A. (2006), *Global change during the Paleocene-Eocene thermal maximum, Rep. 21*, 228 pp., Lab. of Palaeobotany and Palynology Found., Utrecht, Netherlands.

Sluijs, A., H. Brinkhuis, C. E. Stickley, J. Warnaar, G. L. Williams, and M. Fuller (2003), Dinoflagellate cysts from the Eocene/Oligocene transition in the Southern Ocean; results from ODP Leg 189, *Proc. Ocean Drill. Program Sci. Results*, *189*, 1–42.

Sluijs, A., J. Pross, and H. Brinkhuis (2005), From greenhouse to icehouse; organic-walled dinoflagellate cysts as paleoenvironmental indicators in the Paleogene, *Earth Sci. Rev.*, *68*, 281–315.

Sluijs, A., et al. (2006), Subtropical Arctic Ocean temperatures during the Palaeocene/Eocene thermal maximum, *Nature*, *441*, 610–613, doi:10.1038/nature04668.

Sluijs, A., G. J. Bowen, H. Brinkhuis, L. J. Lourens, and E. Thomas (2007a), The Palaeocene-Eocene thermal maximum super greenhouse: Biotic and geochemical signatures, age models and mechanisms of global change, in *Deep Time Perspectives on Climate Change: Marrying the Signal From Computer Models and Biological Proxies*, edited by M. Williams et al., *Geol. Soc. Spec. Publ.*, 347, 323–347.

Sluijs, A., H. Brinkhuis, S. Schouten, S. M. Bohaty, C. M. John, J. C. Zachos, J. S. Sinninghe Damsté, E. M. Crouch, and G. R. Dickens (2007b), Environmental precursors to light carbon input at the Paleocene/Eocene boundary, *Nature*, *450*, 1218–1221, doi:10.1038/nature06400.

Sluijs, A., U. Röhl, S. Schouten, H.-J. Brumsack, F. Sangiorgi, J. S. Sinninghe Damsté, and H. Brinkhuis (2008), Arctic late Paleocene-early Eocene paleoenvironments with special emphasis on the Paleocene-Eocene thermal maximum (Lomonosov Ridge, Integrated Ocean Drilling Program Expedition 302), *Paleoceanography*, *23*, PA1S11, doi:10.1029/2007PA001495.

Speijer, R. P., and A.-M. M. Morsi (2002), Ostracode turnover and sea-level changes associated with the Paleocene-Eocene thermal maximum, *Geology*, *30*, 23–26, doi:10.1130/0091-7613(2002)030<0023:OTASLC>2.0.CO;2.

Speijer, R. P., and B. Schmitz (1998), A benthic foraminiferal record of Paleocene sea level and trophic/redox conditions at Gebel Aweina, Egypt, *Palaeogeogr. Palaeoclimatol. Palaeoecol.*, *137*, 79–101, doi:10.1016/S0031-0182(97)00107-7.

Speijer, R. P., and T. Wagner (2002), Sea-level changes and black shales associated with the late Paleocene thermal maximum: Organic-geochemical and micropaleontologic evidence from the southern Tethyan margin (Egypt-Israel), *Spec. Pap. Geol. Soc. Am.*, *356*, 533–549.

Steckler, M. S., A. B. Watts, and J. A. Thorne (1988), Subsidence and basin modelint at the U.S. Atlantic passive margin, in *The Atlantic Continental Margin*, vol. 1–2, edited by R. E. Sheridan and J. A. Grow, pp. 399–416, Geol. Soc. of Am., Boulder, Colo.

Steurbaut, E. (1998), High-resolution holostratigraphy of middle Paleocene to early Eocene strata in Belgium and adjacent areas, *Palaeontogr. Abt. A*, *247*, 91–156.

Steurbaut, E., R. Magioncalda, C. Dupuis, S. Van Simaeys, E. Roche, and M. Roche (2003), Palynology, paleoenvironments, and organic carbon isotope evolution in lagoonal Paleocene-Eocene boundary settings in North Belgium, in *Causes and Consequences of Globally Warm Climates in the Early Paleogene*, edited by S. L. Wing et al., *Geol. Soc. Am. Spec. Pap.*, 369, 291–317.

Storey, M., R. A. Duncan, and C. C. Swisher III (2007), Paleocene-Eocene thermal maximum and the opening of the Northeast Atlantic, *Science*, *316*, 587–589, doi:10.1126/science.1135274.

Svensen, H., S. Planke, A. Malthe-Sørensen, B. Jamtveit, R. Myklebust, T. R. Eidem, and S. S. Rey (2004), Release of methane from a volcanic basin as a mechanism for initial Eocene global warming, *Nature*, *429*, 542–545, doi:10.1038/nature02566.

Taylor, F. J. R. (Ed.) (1987), *The Biology of Dinoflagellates*, 785 pp., Blackwell Sci., London.

Thomas, D. J., and T. J. Bralower (2005), Sedimentary trace element constraints on the role of North Atlantic Igneous Province volcanism in late Paleocene-early Eocene environmental change, *Mar. Geol.*, *217*, 233–254, doi:10.1016/j.margeo.2005.02.009.

Thomas, D. J., J. C. Zachos, T. J. Bralower, E. Thomas, and S. Bohaty (2002), Warming the fuel for the fire: Evidence for the thermal dissociation of methane hydrate during the Paleocene-Eocene thermal maximum, *Geology*, *30*, 1067–1070, doi:10.1130/0091-7613(2002)030<1067:WTFFTF>2.0.CO;2.

Thomas, E., and N. J. Shackleton (1996), The Palaeocene-Eocene benthic foraminiferal extinction and stable isotope anomalies, in *Correlation of the Early Paleogene in Northwestern Europe*, edited by R. W. O. B. Knox et al., *Geol. Soc. Spec. Publ.*, 101, 401–441.

Torricelli, S., G. Knezaurek, and U. Biffi (2006), Sequence biostratigraphy and paleoenvironmental reconstruction in the early Eocene Figols Group of the Tremp-Graus Basin (south-central Pyrenees, Spain), *Palaeogeogr. Palaeoclimatol. Palaeoecol.*, *232*, 1–35, doi:10.1016/j.palaeo.2005.08.009.

Tripati, A., and H. Elderfield (2005), Deep-sea temperature and circulation changes at the Paleocene-Eocene thermal maximum, *Science*, *308*, 1894–1898, doi:10.1126/science.1109202.

Vail, P. R., R. M. Mitchum Jr., and S. Thompson III (1977), Seismic stratigraphy and global changes of sea level, part 4: Global cycles of relative changes of sea level, *Mem. Am. Assoc. Pet. Geol.*, *26*, 83–89.

van Sickel, W. A., M. A. Kominz, K. G. Miller, and J. V. Browning (2004), Late Cretaceous and Cenozoic sea-level estimates: Backstripping analysis of borehole data, onshore New Jersey, *Basin Res.*, *16*, 451–465, doi:10.1111/j.1365-2117.2004.00242.x.

Wall, D., B. Dale, G. P. Lohmann, and W. K. Smith (1977), The environmental and climatic distribution of dinoflagellate cysts in modern marine sediments from regions in the North and South Atlantic Oceans and adjacent seas, *Mar. Micropaleontol.*, *2*, 121–200, doi:10.1016/0377-8398(77)90008-1.

Westerhold, T., U. Röhl, J. Laskar, I. Raffi, J. Bowles, L. J. Lourens, and J. C. Zachos (2007), On the duration of Magnetochrons C24r and C25n, and the timing of early Eocene global warming events: Implications from the ODP Leg 208 Walvis Ridge depth transect, *Paleoceanography*, *22*, PA2201, doi:10.1029/2006PA001322.

White, R., and D. McKenzie (1989), Magmatism at rift zones: The generation of volcanic continental margins and flood basalts, *J. Geophys. Res.*, *94*, 7685–7729, doi:10.1029/JB094iB06p07685.

Zachos, J. C., K. C. Lohmann, J. C. G. Walker, and S. W. Wise (1993), Abrupt climate change and transient climates during the Palaeogene: A marine perspective, *J. Geol.*, *101*, 191–213.

Zachos, J., M. Pagani, L. Sloan, E. Thomas, and K. Billups (2001), Trends, rhythms, and aberrations in global climate 65 Ma to present, *Science*, *292*, 686–693, doi:10.1126/science.1059412.

Zachos, J. C., M. W. Wara, S. Bohaty, M. L. Delaney, M. R. Petrizzo, A. Brill, T. J. Bralower, and I. Premoli Silva (2003), A transient rise in tropical sea surface temperature during the Paleocene-Eocene thermal maximum, *Science*, *302*, 1551–1554, doi:10.1126/science.1090110.

Zachos, J. C., et al. (2005), Rapid acidification of the ocean during the Paleocene-Eocene thermal maximum, *Science*, *308*, 1611–1615, doi:10.1126/science.1109004.

Zachos, J. C., S. Schouten, S. Bohaty, T. Quattlebaum, A. Sluijs, H. Brinkhuis, S. Gibbs, and T. J. Bralower (2006), Extreme warming of mid-latitude coastal ocean during the Paleocene-Eocene Thermal Maximum: Inferences from TEX86 and Isotope Data, *Geology*, *34*, 737–740, doi:10.1130/G22522.1.

S. M. Bohaty and J. C. Zachos, Earth and Planetary Sciences Department, University of California at Santa Cruz, CA 95060, USA.

H. Brinkhuis, A. F. Lotter, A. Sluijs, and N. L. D. Welters, Palaeoecology, Institute of Environmental Biology, Laboratory of Palaeobotany and Palynology, Utrecht University, Budapestlaan 4, NL-3584 CD Utrecht, Netherlands. (a.sluijs@uu.nl)

E. M. Crouch, GNS Science, P.O. Box 30-368, Lower Hutt, New Zealand.

J. S. Sinninghe Damsté and S. Schouten, Department of Marine Biogeochemistry and Toxicology, Royal Netherlands Institute for Sea Research, P.O. Box 59, NL-1790 AB Den Burg, Texel, Netherlands.

G. R. Dickens, Department of Earth Science, Rice University, 6100 Main Street, Houston, TX 77005, USA.

L. Handley and R. D. Pancost, Bristol Biogeochemistry Research Centre, Organic Geochemistry Unit, School of Chemistry, University of Bristol, Bristol, UK.

C. M. John, Department of Earth Science and Engineering, Imperial College London, London SW7 2BP, UK.

D. Munsterman, Netherlands Institute of Applied Geoscience TNO–National Geological Survey, P.O. Box 80015, NL-3508 TA Utrecht, Netherlands.

G.-J. Reichart, Department of Earth Sciences, Utrecht University, Budapestlaan 4, NL-3584 CD Utrecht, Netherlands.